# Design and Implementation of an Integrated Switched-Oscillator Impulse Generator

by

Samira Mohammadzamani

A Thesis submitted to the Faculty of Graduate Studies of
The University of Manitoba
in partial fulfillment of the requirements of the degree of

Master of Science

Department of Electrical and Computer Engineering
University of Manitoba
Winnipeg, Canada

# Examining Committee

This thesis was examined and approved by the following examining committee on August 23, 2019:

- **Prof. B. Kordi** (advisor)

  Department of Electrical & Computer Engineering

  University of Manitoba

- **Prof. P. Mojabi**

  Department of Electrical & Computer Engineering

  University of Manitoba

- **Prof. D. Swatek**

  Department of Electrical & Computer Engineering

  University of Manitoba

# Abstract

In this thesis, an integrated impulse generator has been designed, simulated, fabricated and tested. The switched-oscillator topology has been used as the impulse generator. A switched oscillator consists of a low impedance transmission line, which charges through a DC source with a large input impedance. The transmission line is connected to a high speed switch at one end and a high feed point impedance antenna at the other end. After charging the transmission line, closing the fast switch short circuits the transmission line, resulting a transient wave propagating toward the antenna. The high mismatch between transmission line characteristic impedance and antenna feed point impedance causes a big reflection at the antenna terminal. Due to the short circuit at switch terminal, the reflected signal will reflect back at the switch terminal as well. These back and forth reflections generates a series of pulses at the antenna terminal which will transmit by the antenna. Switched oscillators are used to generate high power electromagnetic signals in high power microwave applications.

A time domain simulation as well as the sensitivity analysis have been done in this thesis to find the most important design parameters. Three prototype switched oscillator has been designed and fabricated. The first prototype consists of a gas discharge tube as switch, a coaxial cable, and a monopole antenna. In the second prototype, a gas discharge tube as switch, a microstrip transmission line, and a printed circuit board monopole antenna is used. In the third prototype, a conductor-backed coplanar waveguide is used instead of microstrip transmission line. The switched oscillator impulse generator is designed to operate in the industrial, scientific and medical (ISM)

radio frequency band with purpose of being part of the interrogation system of a passive, wireless electric field sensor. An impulse generator with the resonance frequency of 915 MHz and bandwidth of 10 MHz has been designed and fabricated in this project.

# Acknowledgements

First and foremost, I would like to thank my advisor, Dr. Behzad Kordi, for his valuable support and patience during my masters study. His guidance, made me able to find the right path and the discussions that we had always gave me great ideas to overcome all difficulties that I had during my research.

Many thanks to my thesis committee, Dr. Puyan Mojabi and Dr. David Swatek for their comments and suggestions to improve my thesis.

I am truly thankful to Daryl Hamelin, Cory Smit, Zoran Trajkoski for their kind help and practical knowledge to solve the problems we faced during the thesis at the laboratory.

I am also grateful to Alex McIlraith for providing the DC shock circuit and his knowledge which was very useful for my thesis. Many thanks to Manuja Shamith Gunawardana Sooriyaarachchige Don and Amirmasoud Amirkabiri for all the help he provided me for simulating my design.

Financial support from Manitoba Hydro and Canada Natural Sciences and Engineering Research Council (NSERC) is acknowledged. The support from CMC microsystems for providing the simulation software tools is highly appreciated.

The last but not the least, I would like to express my deepest appreciation to my loving family. My sincere gratitude goes to my beloved husband, Ehsan, for being always understanding and caring during my studies. I appreciate his patience for always being amazingly supportive and loving in my most difficult times of studies.

# Dedication

*For my amazing Parents,*

*My wonderful supportive husband,*

*and My dear sisters*

# Table of Contents

# List of Figures

# List of Tables

# Chapter 1

# Introduction

## 1.1 Background

The developing demand for electric power has made the high quality and reliable electric power an essential necessity. Furthermore, the growing reliance on electricity has increased the cost of power outages and quality disturbances. Consequently, to eliminate or decrease the risk of any equipment malfunctions and outages leading to power instability and disturbances, a maintenance system, consisting of online, distributed and low-cost condition monitoring, diagnostics and protection is vital in modern power systems [1]. Additionally, high voltage apparatus induce a high electric field in the surrounding area which makes working with or around these devises extremely hazardous for personnel. Therefore, remote condition monitoring system is in high demand [2].

The conventional method to monitor the condition and performance of high voltage apparatus contains bulky devices that step down the high voltage or high current and measure them with low voltage and current measurement equipment. Employing these equipment inserts some limitation to the measurement results. Furthermore, due to direct attachment of measurement devices power dissipation and source loading is an important drawback of this method. Additionally, these equipment require appropriate insulation from high voltage apparatus which imposes regular

maintenance and extra cost [1–3].

Wireless passive resonator-based electric field sensors have been developed recently in the industrial application. These sensors are passive, that means they do not require any power source and they can be interrogated remotely. These low cost, passive, low weight and wireless sensors propose new advantages compared to conventional measurement methods [4–7].

## 1.2 Problem Definition

The wireless passive resonator-based electric field sensor is a non linearly loaded transmission line resonator with variable resonance frequency. The variation of the magnitude of the to-be-measured external electric field changes the resonance frequency of the sensor. By measuring the resonance frequency of the sensor, the amplitude of the external electric field could be measured. The sensor interrogation system works remotely by sending radio frequency (RF) pulses to the sensor and then receiving the ring-backs of the RF pulses. By analyzing the ring-backs from the sensor, The resonance frequency of the sensor and subsequently the amplitude of the external electric field could be obtained. The main application of these sensors is testing of high voltage power system apparatus. The remote interrogation system and being passive(i.e. no need to power source) made these sensors very advantageous for measurement and inspection of high electric field and high voltage. The current interrogation system employs a pulsed radio frequency (RF) source to excite the sensors [8]. In this thesis, an impulse generator is designed to replace the switched RF source in the interrogation system. Therefore, the control of the center frequency and bandwidth of the RF pulse which excites the sensor will improve and also the configuration of the interrogation system will simplify.

The electric field sensor integrated with the impulse generator are small, light weight, passive and inexpensive which makes it feasible to utilize in distributed measurements around high voltage apparatus to establish an array of sensors. The measurement information of the array of sensors can be employed to acquire electric field characterization of high voltage apparatus. The wireless

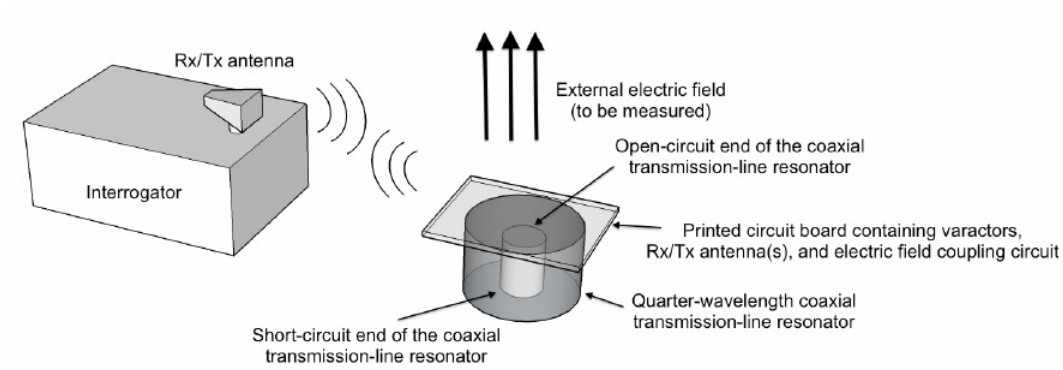


**Fig. 1.1:** An overall diagram of the wireless, passive sensor system. It consist of a quarter wavelength coaxial cavity resonator and a printed circuit board containing varactors.

interrogation system provides remote access to the information of the sensors which eliminate the risk of human resources being exposed to high electric field/high voltage. The sensors are designed to operate in the ISM band at 2.45 GHz with a maximum bandwidth of 100 MHz.

Figure 1.1 shows an overall diagram of the wireless, passive electric field sensor system. The wireless sensor is designed using a coaxial cavity resonator structure, which is capacitively loaded to varactors. Varactor is a type of diode that behaves like a variable capacitor. When the diode is reversed bias its capacitance varies with the voltage applied to it. They are commonly used as a tuning device in RF applications. As Figure 1.1 shows, a printed circuit board on top of the cavity resonator couples the varactor and the external electric field and the external electric field charges the varactor. Capacitance of the varactor varies by the induced charge, therefore the capacitance load of the cavity resonator will change and subsequently the resonant frequency of the resonator will change.

The wireless interrogation system detects the variation in the resonant frequency of the cavity resonator. Figure 1.2 demonstrates the procedure of interrogating the resonator. The remote interrogation system operates by sending the radio frequency (RF) waves to the cavity resonator for a short period of time and afterward receiving the ring back of the RF wave from the resonator.

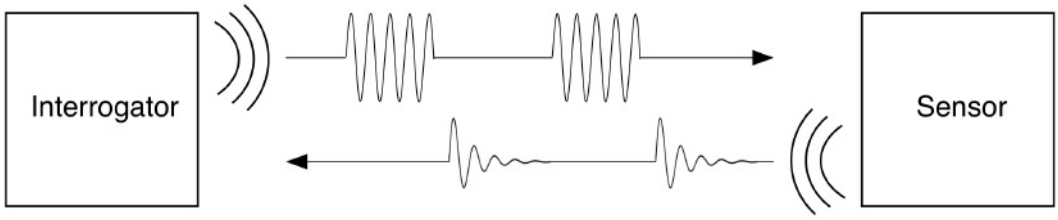


**Fig. 1.2:** A schematic representing the operation of the interrogation system.The interrogator sends RF signals to the cavity resonator and receives the ring back of the signal from the resonator.

In the existing interrogation system, a commercial RF source and an RF switch transmits the RF signals [8]. The goal of this thesis was to design, implement, and test a low cost integrated switched oscillator that will generate pulses whose spectrum cover the required center frequency and bandwidth of the resonator.

## 1.3 Objective of the Thesis

The objective of this research project is to design, fabricate, and test a low cost integrated switched oscillator that will generate pulses whose spectrum cover the required center frequency and bandwidth of the resonator. The design of the switched oscillator includes designing a low characteristic impedance transmission lines structure on a printed circuit board that includes the charging source and impedance as well as the switching electronics. The antenna must be capable of radiating impulses. The final outcome of this project is the impulse generator that will excite the wireless, passive electric field sensors.

## 1.4 Research Contributions

The contributions of this thesis are as follows:

- The switched oscillator has been designed and simulated at 915 MHz.The proposed design is examined precisely by simulation and the features that affect the generated signal criteria are optimized.

- Two successful prototype switched oscillator have been fabricated as a novel wireless pulse generator for the remote interrogation system of the wireless passive electric field sensor.

### 1.4.1 Publications

- The outcome of this study has been submitted as a conference poster to International Conference on Electromagnetic Radiation and Spectrum (ICERS 2019) [9]. The main focus of the paper is on the design, fabrication, and assessment of the switched oscillator based impulse generator for the application in wireless passive electric field sensors using coaxial cables transmission line.

- Another journal paper has been prepared to be submitted to PIERS Letter journal. This paper is discussing the design, simulation and fabrication of the coaxial cable switched oscillator and conductor-backed coplanar waveguide switched oscillator.

## 1.5 Thesis Outline

This thesis is classified into 6 chapters as follows:

**Chapter 1:** Introduction, background information, problem definition, objective of thesis, and contributions.

**Chapter 2:** Discussion on the theoretical background and literature review. Some background on the desired signal and its spectrum has been discussed. Then an introduction on switched oscillator and its possible topologies has been provided. Literature review of this study has been completed on switched oscillator theory and the different experimentally fabricated switched oscillators.

**Chapter 3:** Discussion on the design procedure of the switched oscillator and computer simulation applied to optimize the proposed switched oscillator design.

**Chapter 4:** Discussion on the fabrication of the different prototypes of the switched oscillator and time domain simulation of the proposed prototype.

**Chapter 5:** Discussion on the experimental result of three fabricated switched oscillator prototype and the frequency analysis of the generated signal.

**Chapter 6:** Conclusion of this thesis project, with a discussion on future work.

# Chapter 2

# Theoretical Background and Literature Review

## 2.1 Theoretical Background

This research is carried out to design, fabricate, and test a compact impulse generator which is composed of an integrated resonant switched oscillator and a pulse-radiating antenna.This device should be capable of generating pulses with certain center frequencies and bandwidth. This compact impulse generator will be used in a passive wireless electric field sensor which has been designed and fabricated in a PhD thesis by Dr. Mana Yazdani [8]. This electric field sensor consists of a coaxial cavity resonator, loaded with varactors. Change in electric field varies the capacitance of the varactor and therefore the resonance frequency of the resonator will change. An interrogation system, remotely, sends RF signal toward the resonator and receives the ring backs from the resonator. The impulse generator will be employed in the interrogation system of the electric field sensor.

To interrogate the cavity resonator, the integrated switched oscillator requires to transmit a waveform to the resonator. The desired waveform is a sine wave modulated by a pulse waveform, similar to that showing Figure 2.1a. The frequency spectrum of such signal is demonstrated in Figure 2.1b.

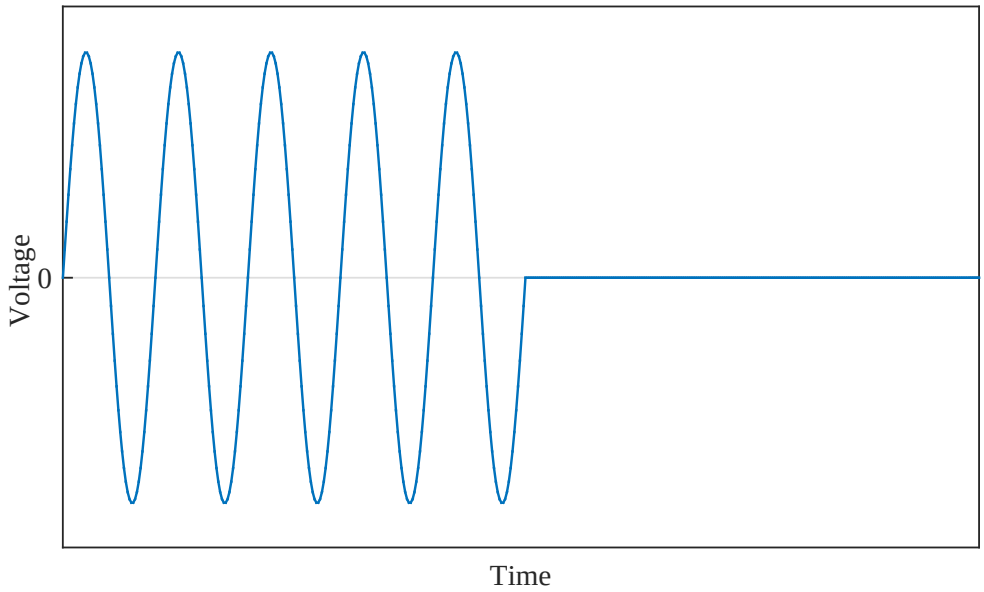


**(a)**

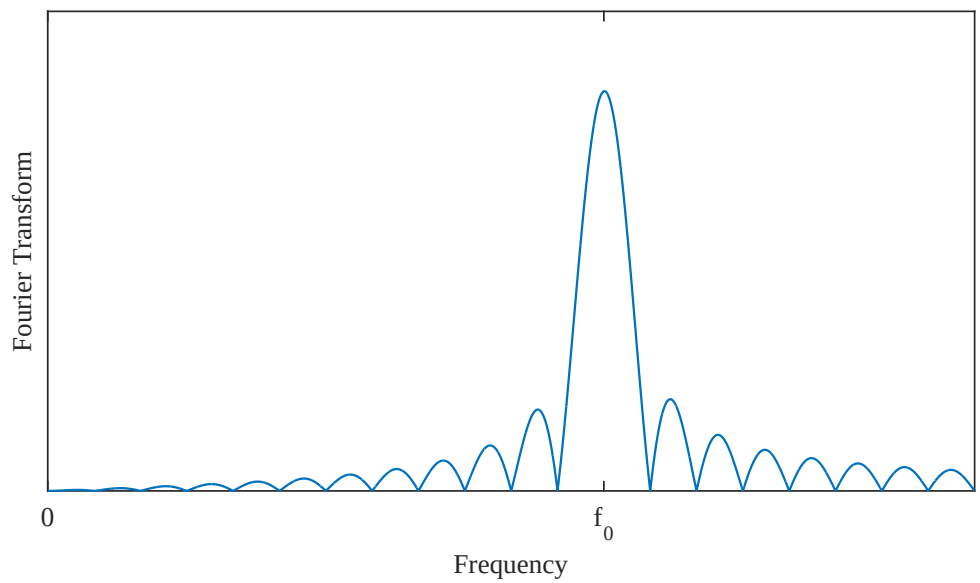


**(b)**

**Fig. 2.1:** The desired signal to interrogate the system(a) and its frequency spectrum (b).

The time domain waveform and the frequency spectrum of a signal, that is expected from a switched oscillator is demonstrated in Figure 2.2. As it is indicating from Figure 2.2, the spectrum of the signal, generated by a switched oscillator is reasonably similar to the desired signal spectrum. The spectrum of the switched oscillator includes the dominant section of the desired signal spectrum. Therefore, the switched oscillator signal met the requirements of the interrogation system.

The time domain representation of the signal generated by the switched oscillator is:

$$f(t) = \sin \omega_0 t \; e^{-\alpha t} u(t) \tag{2.1}$$

where $\omega_0$ is the center frequency of the signal and $\alpha$ is the damping coefficient. To determine the center frequency and bandwidth of the generated signal, the frequency analysis of the generated signal has been employed. The Fourier transform of the generated signal, $f(t)$ is given by

$$\begin{aligned} F(j\omega) &= \frac{\omega_0}{{\omega_0}^2 + (\alpha + j\omega)^2} \\ &= \frac{\omega_0}{({\omega_0}^2 + \alpha^2 - \omega^2) + 2j\alpha\omega} \end{aligned} \tag{2.2}$$

The magnitude of the Fourier transform of the generated signal is:

$$\begin{aligned} |F(j\omega)| &= \frac{\omega_0}{\sqrt{({\omega_0}^2 + \alpha^2 - \omega^2)^2 + 4\alpha^2\omega^2}} \\ &= \frac{\omega_0}{\sqrt{{\omega_0}^4 + \alpha^4 + \omega^4 - 2{\omega_0}^2\omega^2 + 2\alpha^2\omega^2}} \\ &= \frac{\omega_0}{\sqrt{({\omega_0}^2 + \alpha^2)^2 + \omega^2(\omega^2 - 2{\omega_0}^2 + 2\alpha^2)}} \end{aligned} \tag{2.3}$$

The Fourier transform magnitude peaks at $\omega_0$ and the peak magnitude would be:

$$|F_{max}| = |F(j\omega_0)| = \frac{\omega_0}{\alpha^2\sqrt{\alpha^2 + 4{\omega_0}^2}} \tag{2.4}$$

The cut-off frequencies are where the magnitude of the Fourier transform of the signal is at 0.7 times its maximum value

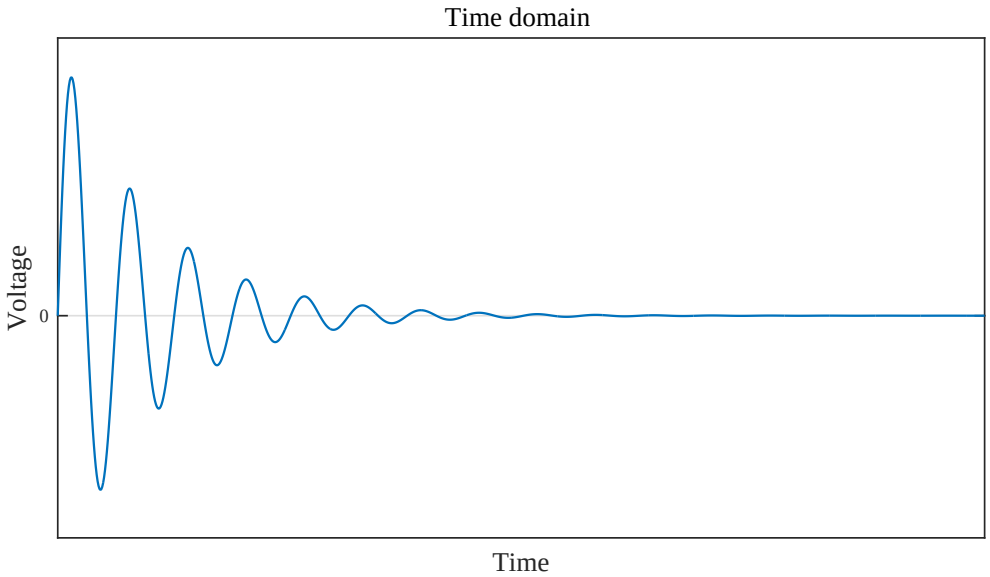


**(a)**

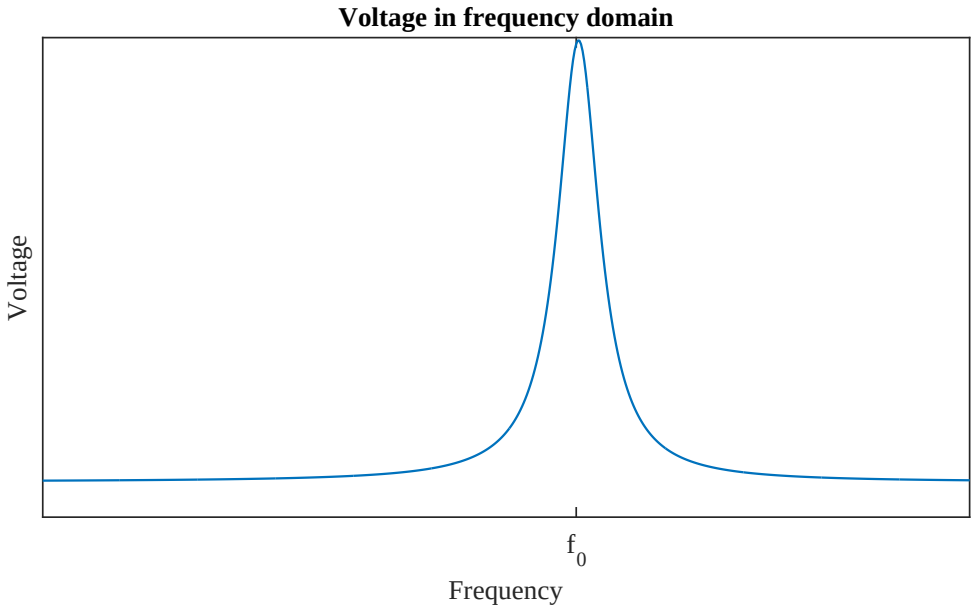


**(b)**

**Fig. 2.2:** Time domain and frequency domain representation of a signal generated by a switched oscillator.

$$|F(j\omega)| = 0.7|F_{max}|. \tag{2.5}$$

Equation 2.5 leads to a forth order polynomial equation and by solving this equation, the cut-off frequencies are found as

$$\omega_1 = \sqrt{{\omega_0}^2 - \alpha^2(1 + 0.5\alpha\sqrt{23.28{\omega_0}^2 + 8.32\alpha^2})} \tag{2.6a}$$

$$\omega_2 = \sqrt{{\omega_0}^2 - \alpha^2(1 - 0.5\alpha\sqrt{23.28{\omega_0}^2 + 8.32\alpha^2})} \tag{2.6b}$$

Therefore, the bandwidth of the signal is calculated using

$$BW = \omega_1 - \omega_2 \tag{2.7}$$

An example signal of $\sin\omega_0 t\ e^{-\alpha t}u(t)$ at $\omega_0 = 915$ MHz and $\alpha = 8 \times 10^7$ is represented in Figure 2.3a. Signal continues for about 60 ns. The magnitude of the Fourier transform of the signal computed by MATLAB depicted in 2.3b. The center frequency and the bandwidth of the Fourier transform of the signal matches with the values calculated by 2.7 and 2.6b. The results from the MATLAB Fourier transform computation and (2.6b) are presented in Table 2.1.

**Table 2.1:** Comparing results from MATLAB Fourier transform computation of $\omega_1$ and $\omega_2$ and values computed by (2.6a)

| Cut_off Frequency | $\omega_1$(MHz) | $\omega_2$(MHz) | BW(MHz) |
|---|---|---|---|
| Value Computed by Matlab | 929.23 | 900.36 | 28.87 |
| Value Computed by Equation(2.6a) | 931.88 | 896.12 | 35.76 |

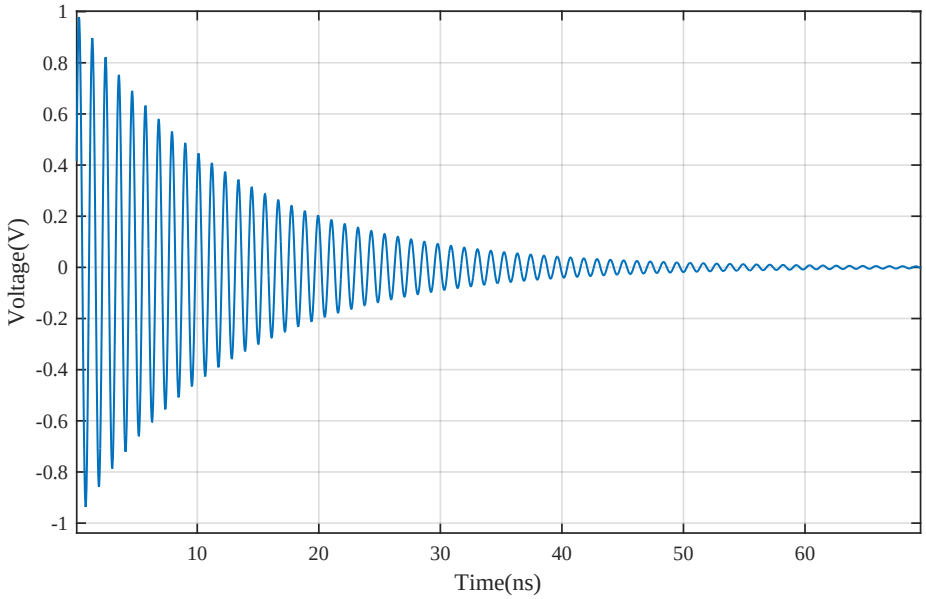


**(a)**

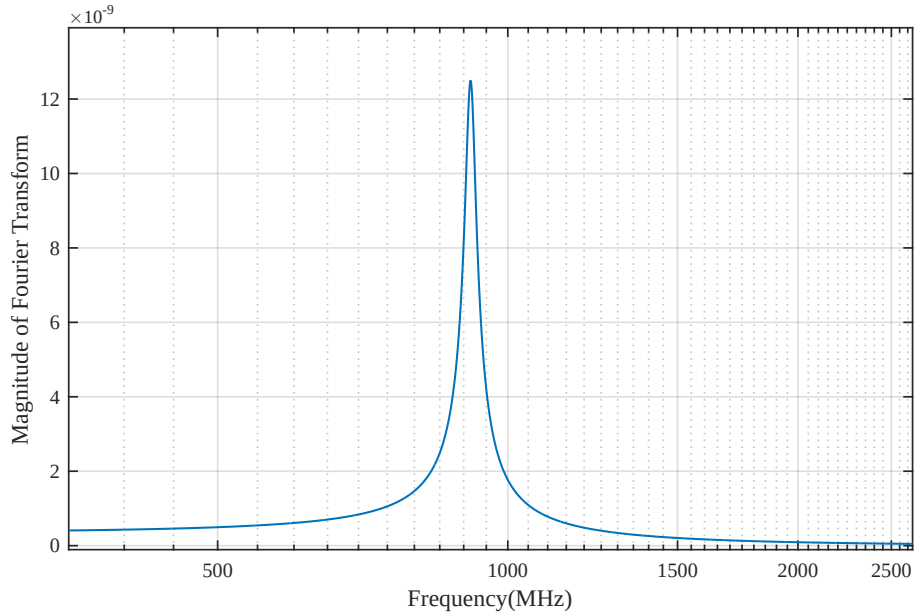


**(b)**

**Fig. 2.3:** Simulation result of a switched oscillator with resonance frequency of 915 MHz (a) Time domain result (b) Frequency domain result.

## 2.2 Introduction to Transmission Line Theory

Lumped element model of a transmission line section with length of Δz is presented in Figure 2.4. R is per unit length series resistance, L is per unit length series inductance, G is per unit length shunt conductance, and C is per unit length shunt capacitance [10].

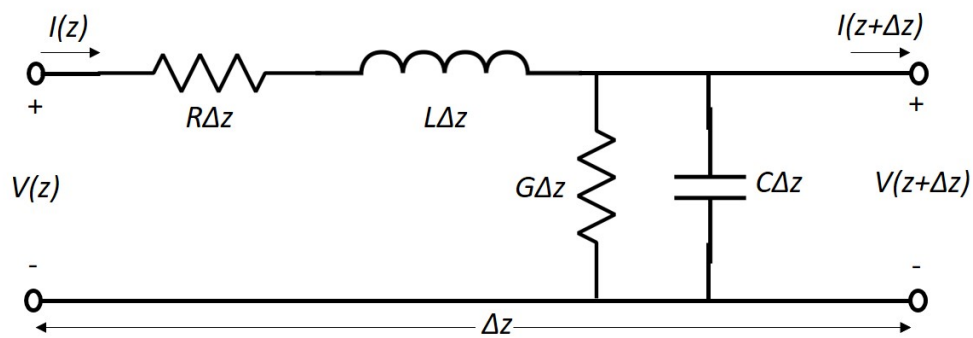


**Fig. 2.4:** Lumped element model of a transmission line section with length of Δz [10].

The series voltage drop (ΔV), along the line section with current I, is

$$\Delta V = -(R + j\omega L)\Delta z I \tag{2.8}$$

where $R + j\omega L$ is the impedance of the line. If Δz→0 then

$$\frac{dV}{dz} = -(R + j\omega L)I \tag{2.9}$$

The shunt current ΔI flowing across the line section with the voltage of V is

$$\Delta I = -(G + j\omega C)\Delta z V \tag{2.10}$$

where $G + j\omega C$ is the impedance of the line. If $\Delta$z$\rightarrow$0 then

$$\frac{dI}{dz} = -(G + j\omega C)V \tag{2.11}$$

Equations 2.9 and 2.11 can lead to wave equations:

$$\frac{d^2V}{dz^2} - \gamma^2 V = 0, \tag{2.12a}$$

$$\frac{d^2I}{dz^2} - \gamma^2 I = 0, \tag{2.12b}$$

where

$$\gamma = \alpha + j\beta = \sqrt{(R + j\omega L)(G + j\omega C)} \tag{2.13}$$

is the propagation constant.

Solving equations 2.12a and 2.12b results in

$$V(z) = {V_0}^+ e^{-\gamma z} + {V_0}^- e^{\gamma z}, \tag{2.14a}$$

$$I(z) = {I_0}^+ e^{-\gamma z} + {I_0}^- e^{\gamma z}, \tag{2.14b}$$

where $e^{-\gamma z}$ represents wave propagation in +z direction, and $e^{\gamma z}$ represents wave propagation in $-$z direction. Applying equation 2.9 to equation 2.14a results in

$$I(z) = \frac{\gamma}{R + j\omega L}({V_0}^+ e^{-\gamma z} + {V_0}^- e^{\gamma z}). \tag{2.15}$$

Therefore, "characteristic impedance", $Z_0$, can be defined as

$$Z_0 = \frac{R + j\omega L}{\gamma} = \sqrt{\frac{R + j\omega L}{G + j\omega C}} \tag{2.16}$$

## 2.3 Literature Review

The fundamentals of Switched Oscillators first was introduced by C. E. Baum in 2000 [11]. A Switched Oscillators consists of a low impedance transmission line ($Z_0$) charged by a DC source ($V_{DC}$) through large impedance ($Z_S$) at desired frequencies (to block any effect of DC source on the signal) and terminated to a high impedance antenna ($Z_A$) at one end and a fast closing switch ($S$) at the other end. The DC block capacitor (C) prevents any DC signal to go through the antenna. The general schematic of a switched oscillator is presented in Figure 2.5.

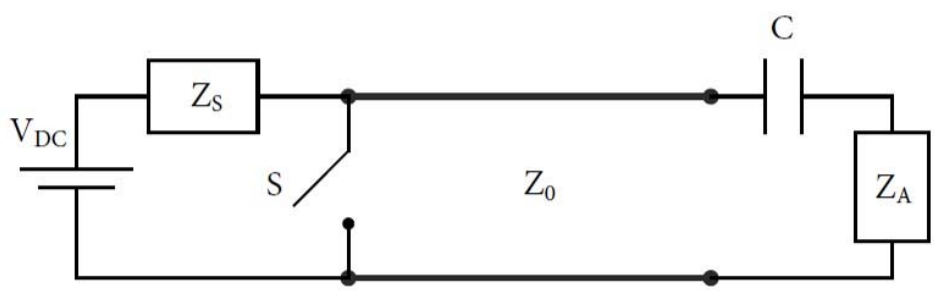


**Fig. 2.5:** Schematic of a switched oscillator [11].

Once the line is charged, the switch S will close and short-circuit the transmission line. Therefore, a fast transient will be generated and travels along the transmission line. Because of the mismatch between the antenna and the transmission line, only a part of fast transient wave will be radiated and a portion of the fast transient wave will reflect back. At the other end of the transmission line, there is a closed switch. Consequently, a second reflection with reversed sign will propagate towards the antenna and the wave continues reflecting back and forth. Hence, at the terminal of antenna, there will be a series of positive and negative pulses with descending amplitude.

### 2.3.1 Quarter Wavelength Switched Oscillator

The quarter wavelength switched oscillator includes a charged quarter wavelength ($\lambda/4$) transmission line terminated by a high impedance antenna at one end and a switch at the other end. Figure 2.6 demonstrates two configuration for the quarter wavelength switched oscillators: a) differential and b) single ended.

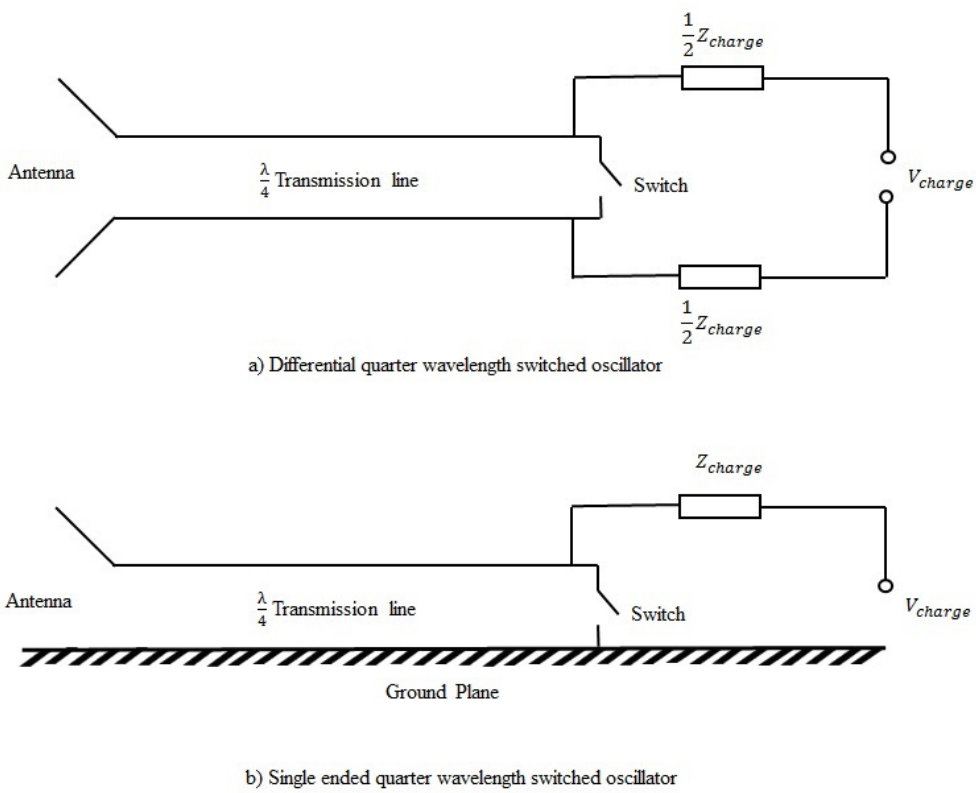


**Fig. 2.6:** Schematic of a) differential and b) single ended quarter wavelength switched oscillator. [11]

Upon closing the switch, a fast transient wave propagates toward the antenna and reflects back and forth generating a waveform The center frequency of these pulses is determined by the the length of transmission line, as each cycle of the generated pulse is equal to 4 times the delay of the transmission line [12]. Therefore, The center frequency is given by

$$\begin{aligned} f_c &= \frac{1}{4t_t} \\ &= \frac{v_p}{4L} \end{aligned} \tag{2.17}$$

where $t_t$ is the transient time of the transmission line, $v_p$ is the propagation velocity and $L$ is the length of transmission line.

The reflection coefficient at the terminal of the antenna is:

$$\Gamma = \frac{1 - \dfrac{Z_0}{Z_A}}{1 + \dfrac{Z_0}{Z_A}} \tag{2.18}$$

where $Z_0$ is the quarter wavelength transmission line characteristic impedance and $Z_A$ is the input impedance of the antenna. Since $Z_0 \ll Z_A$, using Taylor series, the reflection coefficient will become

$$\Gamma \simeq 1 - 2\frac{Z_0}{Z_A} \tag{2.19}$$

On the assumption that the switch is ideal and remains closed while the wave is reflecting back toward switch, the reflection coefficient at the switch terminal would be -1. Therefore, the amplitude of the second wave reflecting from the antenna would be $\Gamma^2$ times the amplitude of the first wave. The wave continues back and forth with the decreasing amplitude. The rate of decrease in amplitude would be $-\Gamma$. Consequently, the amplitude of the $N^{th}$ cycle would be $\Gamma^{2N}$. If the amplitude of the Nth cycle set to $e^{-1}$, thus N will be:

$$N = -\frac{1}{2\ln\Gamma} \tag{2.20}$$

which N is the effective number of cycles. Using (2.18) and Taylor series, N will be

$$N \simeq -\frac{1}{4}\frac{Z_0}{Z_A} \tag{2.21}$$

then the quality factor (Q), describing the rate of damping, can be define as

$$Q = \pi N \tag{2.22}$$

that is the number of radians which the amplitude of the wave at antenna terminal reduce to $e^{-1}$ [13]. Using (2.21) and (2.22) the number of the cycles with the magnitude greater than $e^{-1}$ can be calculated and therefore the duration of the signal can be obtained.

### 2.3.2 Half Wavelength Switched Oscillator

Another suggested design (by [11]) of the switched oscillator is the half wavelength transmission line switched oscillator which consists of a ring shaped transmission line. The circumference of the ring shaped transmission line is $\lambda/2$. Figure 2.7 demonstrates the configuration of a ring shape switched oscillator. This half wavelength switched oscillator can be regarded as two quarter wavelength transmission line with characteristic impedance of $Z_0$, both feeding the antenna equally. The equivalent characteristic impedance of these two transmission line would be $Z_0/2$. The advantage of this configuration is that, the length of the transmission line is doubled for a given frequency, therefore the stored energy available to antenna is twice.

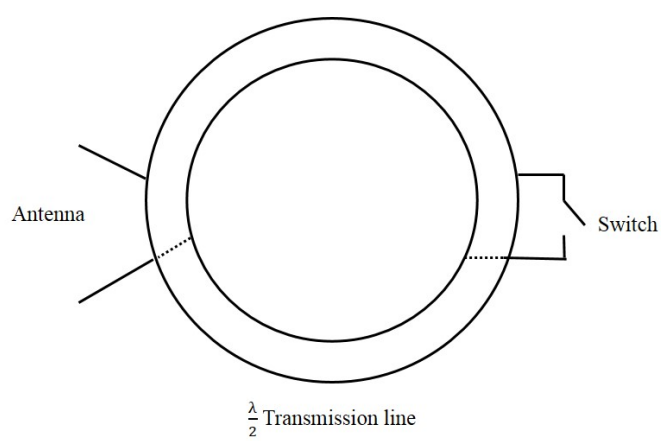


**Fig. 2.7:** Schematic of a ring shaped half wavelength switched oscillator. [11]

## 2.4 Experimental Implementations of Switched Oscillator

The idea of the switched oscillator presented by Baum has been appealing because of its simplicity and its application in high-power mesoband electromagnetic radiators [14]. Baum extended his idea in [15, 16] by introducing the differential switched oscillator and their associated antennas for application in both linear polarization and circular polarization with the aim to increase the voltage delivery to antenna and consequently higher radiated electric field at the far field.

An alternative approach to fabricate the switched oscillator employing the lumped elements suitable for low frequency application has been discussed in [17]. This switched oscillator includes a lumped element inductor and a lumped element capacitor instead of transmission line. According to (2.17), the length of the transmission line determines the frequency of the oscillation of the switched oscillator. Therefor, for lower frequencies, longer transmission line is required. For very low frequencies the length of the transmission line could make the structure of the switched oscillator, physically unstable. A lumped element switched oscillator could be an alternative solution for lower frequencies. Figure 2.8 represents a lumped elements transmission line in a switched oscillator. $L$ and $C$ are per length inductor and capacitor, respectively, and $\Delta z$ is the length increment. Using lumped elements switched oscillator has the high frequency limitation as the wavelength reduces toward the $\Delta z$.

A high efficiency double-folded horn antenna design has been introduced in [18] for differential switched oscillator. In [19] extended design options has been demonstrated by using more complex topologies. These topologies contain multi-axial structures which allows longer transmission line

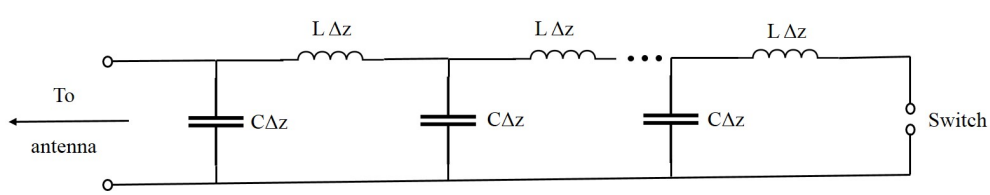


**Fig. 2.8:** Schematic of a lumped elements transmission line as part of a switched oscillator. [17]

length for a given frequency (up to a full wavelength).

In [20], M.Armanious presented important design parameters of a quarter wavelength switched oscillator and using these parameters designed a tunable quarter wavelength switched oscillator that the output can be altered by small, feasible changes in the system. Some of the successful implementation of the switched oscillator concept has been reported in the following.

A method to investigate and analyze the behavior of the coaxial cable switched oscillator has been introduced in [21]. In this method, using chain parameter representation of the system, a semi-analytical solution to design and optimization of the coaxial cable switched oscillators has been presented.

Some examples of successful implementation of the switched oscillator has been reported in following. A recent design of a switched oscillator has been implemented in a Ph.D. thesis by Jose Felix Vega [12]. In this design, a short-circuited coaxial transmission and an air gap that operates as the switch has been employed. A simple monopole antenna has been employed as the impulse radiator. The spectrum of radiated electromagnetic wave is centered at 433 MHz for high power applications.

In [22], the design process and fabrication of switched oscillators integrated with helical antennas has been presented. Two coaxial switched oscillator at 200 MHz and 500 MHz, with gas spark switch and charging voltage of 30 kV has been fabricated and tested.

The investigation of a compact coaxial cable switched oscillator has been reported in [23]. This coaxial cable switched oscillator can reach up to 200 KV at frequency of 600 MHz using a pressurized nitrogen spark gap, a fast charging source and a short helical antenna.

## 2.5 Proposed Impulse Generator

The proposed impulse generator is a quarter wavelength switched oscillator operating at 915 MHz (ISM band). The initial goal was to design and fabricate a quarter wavelength switched oscillator at 2.45 GHz, but the size of the quarter wavelength transmission line at 2.45 GHz is very small,

also to fabricate a 2.45 GHz switched oscillator a very fast switch is needed. Because of difficulties of fabricating such a small transmission line and finding a fast enough switch, 915 MHz switched oscillator has been considered. The quarter wavelength switched oscillator consists of a quarter wavelength transmission line at 915 MHz with low characteristic impedance, an antenna with the resonance frequency around 915 MHz and higher input impedance (with respect to transmission line characteristic impedance), a fast switch and a DC source to charge the transmission line. This proposed quarter wavelength switched oscillator is part of the interrogation system of a passive wireless high electric field sensor.

The proposed switched oscillator has the following advantages for the wireless high electric field sensor interrogation system:

- The proposed switched oscillator is a wireless impulse generator with the capability of remote interrogation of electric field sensor
- The proposed switched oscillator is compact, that means all components of the switched oscillator will be on a printed circuit board.
- The proposed switched oscillator is relatively small and light weight compare to existing impulse generators.
- The fabrication procedure is relatively inexpensive and the proposed switched oscillator is capable of being available commercially which is a key characteristic for mass production of the electric field sensor.

# Chapter 3

# Design and Simulation of the Switched Oscillator

Design and simulation of the proposed quarter wavelength switched oscillator is presented in this chapter. A switched oscillator has been designed as a wave generator to be a part of an interrogation system of a passive electric field sensor. The switched oscillator is composed of a quarter wavelength transmission line, terminating to a fast closing switch at one end and a high impedance antenna at the other end. The resonance frequency of the switched oscillator is determined by the length of the transmission line. First, the switched oscillator structure is discussed. Then, the numerical simulation is used to optimize the characteristics of the design, and the results of the simulations are reported in this chapter. Finally, optimized values of the design dimensions are presented.

## 3.1 Design Criteria

The proposed switched oscillator has been designed to generate a pulse waveform with a decreasing amplitude at a certain center frequency which is shown in Figure 2.1b. Therefore, the center frequency of the signal and the number of pulses are the two most important criteria to be considered.

### 3.1.1 Center Frequency of the Signal

In Chapter 2.3, it was discussed that, the center frequency of the switched oscillator is the function of the length of the transmission line, given by

$$f_c = \frac{v_p}{4L} \tag{3.1}$$

where $v_p$ is the propagation velocity and $L$ is the length of transmission line.

### 3.1.2 Duration of the Signal

The amplitude of the generated signal by the switched oscillator and subsequently number of the pulses and duration of the signal is predominantly affected by the mismatch at the antenna terminal. By closing the switch, the generated transient signal propagates toward the antenna and reflects back with the reflection coefficient of

$$\Gamma = \frac{V^-}{V^+} = \frac{Z_A - Z_0}{Z_A + Z_0} \tag{3.2}$$

where $Z_0$ is the transmission line characteristic impedance and $Z_A$ is the input impedance of the antenna. $V^+$ is the wave propagating toward the antenna and $V^-$ is the reflected wave at the antenna terminal. Therefore, the more the difference between the characteristic impedance of the transmission line and the feed point impedance of the antenna, the higher the reflection coefficient and consequently the higher the amplitude of the reflected signal. Ideally, the switch impedance is zero and subsequently, the reflection coefficient is -1. Therefore, a signal with the reversed sign reflects from the switch. Technically, the impedance of switch when at closed state is never zero and the reflection coefficient at the switch terminal determines the amplitude of the reversed reflection. Correspondingly, to have higher reflection coefficient and subsequently higher amplitude signal, the difference between the characteristic impedance of the transmission line and the closed state impedance of the switch requires to be the maximum possible value.

## 3.2 Design Procedure

The switched oscillator consists of a DC charging circuit, a switch, a quarter wavelength transmission line and an antenna. The design procedure of each element will be provided in the following.

### 3.2.1 DC Charging Circuit

The DC source charges the transmission line and then the switch will close. In order to eliminate any subsequent effect of the DC source on the generated signal, a large impedance at DC source would be beneficial. This large impedance could be a large resistor or an inductor with high impedance at the center frequency of the switched oscillator.

### 3.2.2 Switch

The switch short circuits the transmission line after charging. Ideally, the impedance of switch at open state must be infinity and the impedance of the switch at close state must be zero. Also it is desired that switch remains closed, during the propagation of the signal through the transmission line. The transition time of the switch must be less than the traveling time that transient signal passes through the transmission line and reflects back to the switch. Otherwise, the wave reaching to the switch encounters different impedance at each half cycle and it causes inaccuracy.

$$t_{\text{transition time}} < \frac{1}{2f_0} \tag{3.3}$$

where $t_{transitiontime}$ is the switch transition time and $f_0$ is center frequency of switched oscillator. Therefore, to design a switched oscillator with the resonance frequency of 915 MHz, the transition time of the switch, ideally, needs to be less than 546 psec.

### 3.2.3 Transmission Line

As it was discussed in Section 2.3, the length of the transmission line determines the resonance frequency of the transmission line. According to (3.1), to design a switched oscillator with the resonance frequency of 915 MHz, the length of the transmission line with the dielectric constant of $\varepsilon_r = 2.02$ requires to be 5.76 cm. According to Section 3.1.2, to have a higher amplitude of the signal, the characteristic impedance of the transmission line requires to be smaller than the feed point impedance of the antenna. Because of the fabrication limitation, the characteristic impedance of the transmission line has chosen to be 15 Ω .

### 3.2.4 Antenna

The first resonance frequency of the antenna requires to be designed at the center frequency of the desired signal. Also as it was discussed in Section 3.1.2 to have a high number of pulse repetition, the input impedance of the antenna needs to be considerably larger than the characteristic impedance of the transmission line. Due to feasible modeling for simulation and ease of fabrication a monopole antenna with the first resonance frequency of 915 MHz and input impedance of 34 Ω has been chosen.

## 3.3 Time Domain Simulation of the Switched Oscillator

The time-domain simulation has been performed by modeling the switched oscillator using PSCAD software. Figure 3.1 represents the schematic of the simulated switched oscillator in the PSCAD software. DC charging circuit has been modeled as a DC source with the amplitude of 10 V and internal resistance of 50 Ω. The internal resistance has been chosen a small value to decrease the simulation running time and a timed breaker has been added to eliminate the effect of the DC source on the generated wave by the switched oscillator after closing the switch. The timed breaker is short circuit at the start of the simulation and after the transmission line has been charged, will

switch to open circuit, to disconnect the DC source from the rest of the circuit.

The switch has been modeled as a variable resistor with the initial resistance of 1 MΩ which is the open state of the switch. After the transmission line has been charged, the resistance of the variable resistance changes linearly to $10^{-6}\Omega$ which is the close state of the switch. The transition time of the variable resistance is 100 ps. Figure 3.2a demonstrates the schematic of the variable resistor control panel and figure 3.2b shows the resistance of the variable resistor over time. The transmission line has been modeled as a coaxial cable line with the length of 5.8 cm and the characteristic impedance of 15 Ω. As the antenna model, an equivalent circuit model with the impedance equivalent to the input impedance of the antenna has been used. The details on the circuit modeling has been reported in the following. The output voltage has been measured at the antenna feed point.

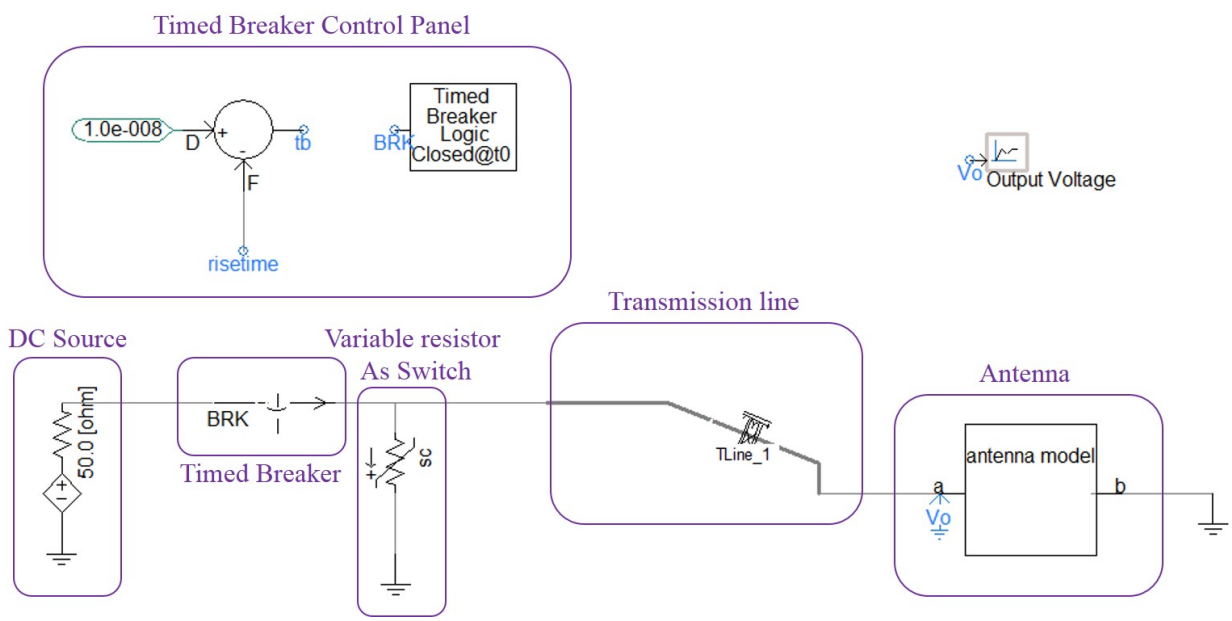


**Fig. 3.1:** Schematice of the simulated switched oscillator using PSCAD software.

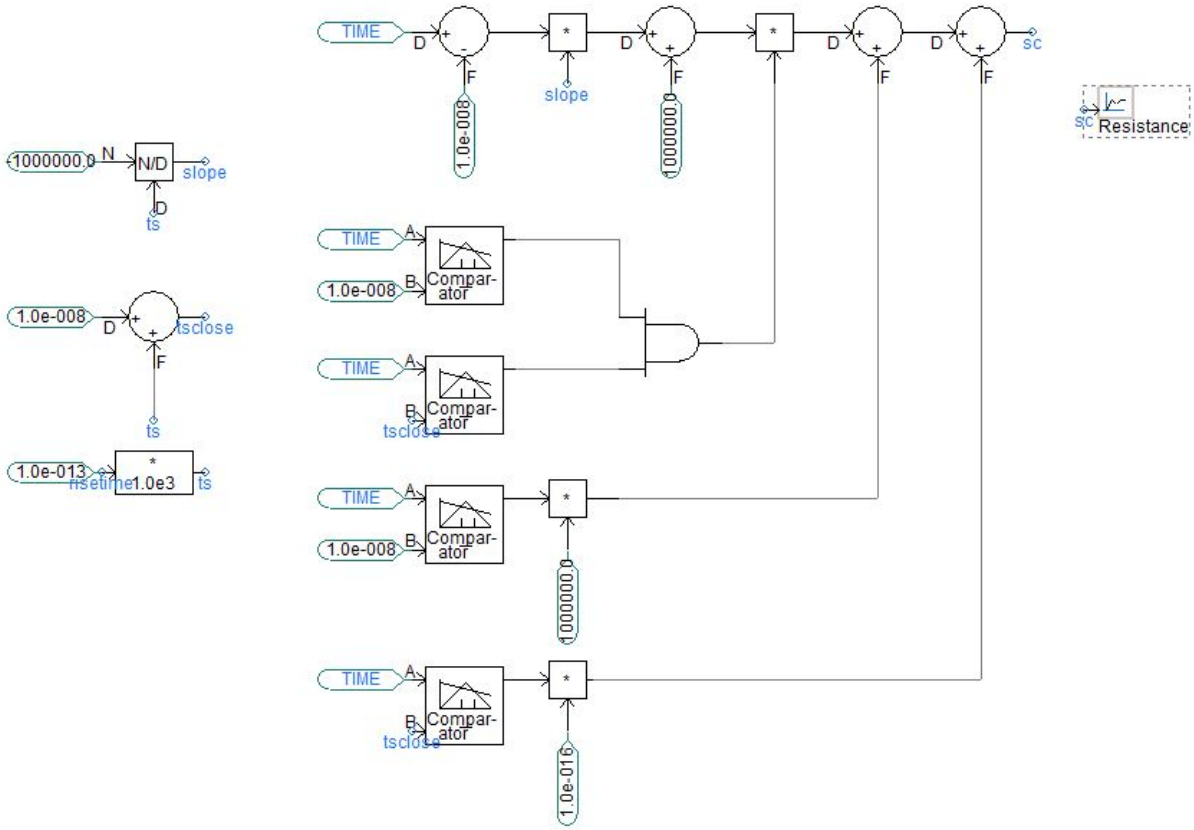


**(a)**

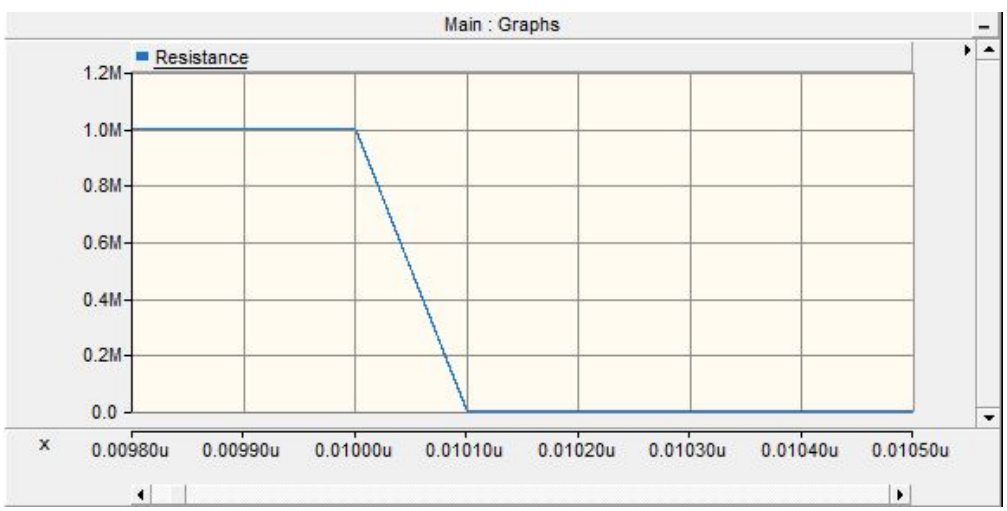


**(b)**

**Fig. 3.2:** (a) Schematice of the variable resistor control panel used as the fast switch in switched oscillator using PSCAD software (b) Switch resistance ($\Omega$) vs time ($\mu s$).

To model the feed point impedance of the antenna in the simulation, circuit synthesis method has been used. Circuit synthesis is a method to obtain an equivalent of the impedance component of a network. The equivalent circuit of a system can be achieved from the frequency response of the system. In our case the frequency response would be the state space model of the input admittance,Y, which can be approximated by [24–26]

$$Y(s) \cong \sum_{m=1}^{n} \frac{R_m}{s - a_m} + D + sE \tag{3.4}$$

In this representation, term $a_m$ is poles of the input admittance, term $R_m$ is residues of the input admittance, term D is shunt conductance and term E is shunt capacitance. Circuit models must be developed for the poles and residues. The equivalent circuit for each real pole and residue would be a RL circuit which is presented in figure 3.3.

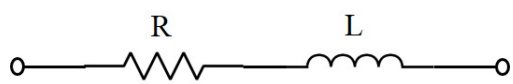


**Fig. 3.3:** RL series circuit.

The values for resistor and inductor can be calculated by [27]

$$L = \frac{1}{R_m} \tag{3.5a}$$

$$R = \frac{-a_m}{R_m} \tag{3.5b}$$

Each complex pole and residue pair can be modeled by an RLC series circuit which is presented in figure 3.4

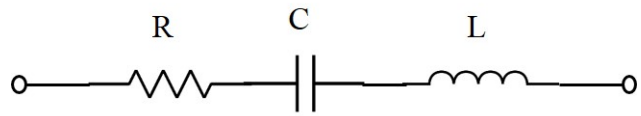


**Fig. 3.4:** RLC series circuit.

Let assume $a_{m1}$ and $R_{m1}$ be a complex pole and residue and $a_{m2}$ and $R_{m2}$ be its conjugate. Therefore, the circuit model elements, R, L, C can be calculated by [27]:

$$L = \frac{1}{R_{m1} + R_{m2}} \tag{3.6a}$$

$$R = \frac{-(a_{m1} + a_{m2})}{R_{m1} + R_{m2}} \tag{3.6b}$$

$$C = \frac{R_{m1} + R_{m2}}{a_{m1}.a_{m2}} \tag{3.6c}$$

Therefore, employing circuit synthesis method, each real pole and residue results in a RL series circuit branch and each complex pole and residue and its conjugate develops a RLC series circuit branch and the number of branches in the equivalent circuit model depends on number of poles and residues.

Consequently, to acquire circuit synthesis method, the feed point impedance of the antenna is required. The feed point impedance of a $\frac{\lambda}{4}$ monopole antenna has been calculated as given by [28]

$$Z_{\text{in}}(\text{monopole}) = \frac{1}{2} Z_{in}(\text{dipole}) = \frac{1}{2}(R_{\text{in}} + jX_{\text{in}}) \tag{3.7}$$

where $R_{in}$ and $X_{in}$ are respectively real part and imaginary part of the feed point impedance of a

$\frac{\lambda}{2}$ dipole antenna and can be calculated by the following equations [28]:

$$R_{in} = \frac{\eta}{2\pi \sin^2(\frac{k\ell}{2})} \Big\{ \gamma + \ln(k\ell) - Ci(k\ell) + \frac{1}{2}\sin(k\ell)[Si(2k\ell) - 2Si(k\ell)] + \frac{1}{2}\cos(k\ell)[C + \ln(\frac{k\ell}{2}) + Ci(2k\ell) - 2Ci(k\ell)] \Big\} \tag{3.8a}$$

$$X_{in} = \frac{\eta}{4\pi \sin^2(\frac{k\ell}{2})} \{ Si(k\ell) + \cos(k\ell)[2Si(k\ell) - Si(2k\ell)] - \sin(k\ell)[2Ci(k\ell) - Ci(2k\ell) - Ci(\frac{2ka^2}{\ell})] \Big\} \tag{3.8b}$$

Where $\eta = \sqrt{\frac{\mu}{\varepsilon}}$ is the characteristic impedance of the medium, $\ell$ is the full length of the dipole, $k$ is the wavenumber equal to $\frac{\lambda}{2\pi}$, $a$ is the radius of the antenna wire, $\gamma = 0.5772$ (Euler's constant) and Ci(x) and Si(x) are the cosine and sine integrals given by:

$$Ci(x) = \int_{-\infty}^{x} \frac{cos(y)}{y}\, \mathrm{d}y \tag{3.9}$$

$$Si(x) = \int_{0}^{x} \frac{sin(y)}{y}\, \mathrm{d}y \tag{3.10}$$

Figure 3.5 demonstrates the real part and imaginary part of the feed point impedance of the monopole antenna with length of 8 cm. This monopole antenna resonance at 915 MHz and the real part and imaginary part of the feed point impedance of the monopole antenna at 915 MHz are respectively 34.16 Ω and 0.000227 Ω.

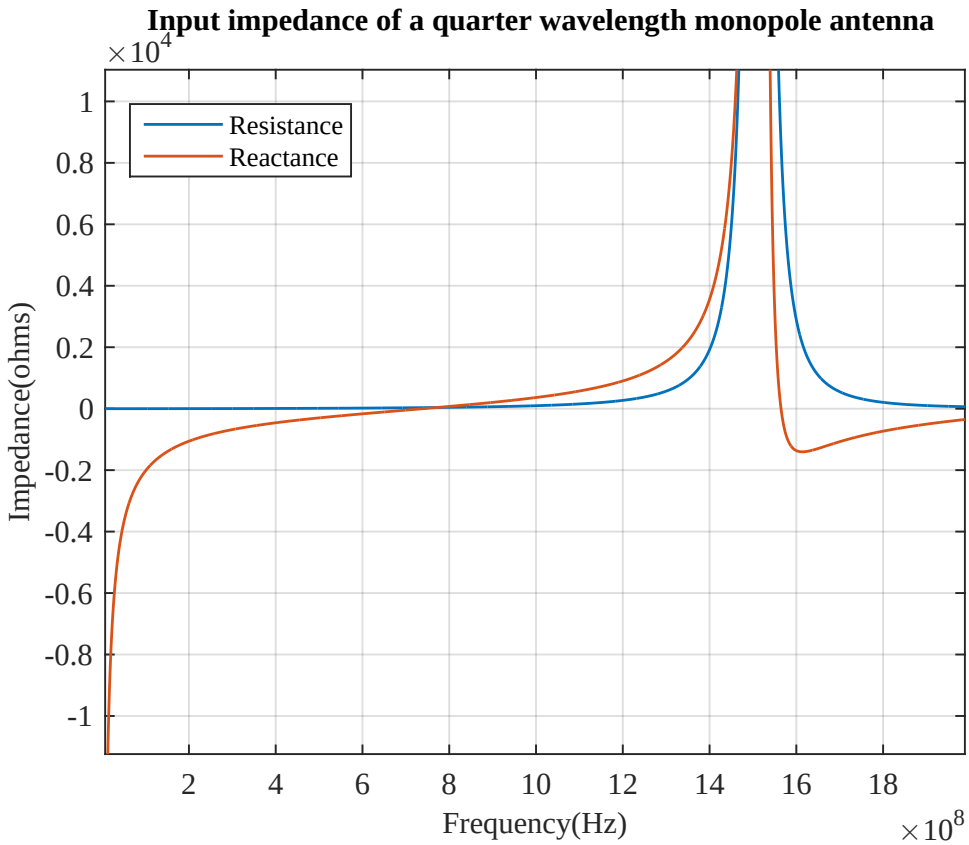


**Fig. 3.5:** real part and imaginary part of the feed point impedance of the monopole antenna.

The Vector Fitting method [29] has been used to find the poles and residues of the closest frequency response approximation that can be fitted to the feed point admittance of the monopole antenna. The Vector Fitting Algorithm is a pole relocating method that the location of poles improves by an iterative process. In this algorithm, a linear problem is solved repeatedly until reaching convergence [29, 30]. The Vector Fitting method identifies the poles ($a_m$), residues ($R_m$), and terms D and E of the least squares problem. The vector fitting is done over the frequency range of 0-2 GHz. The magnitude and phase of the admittance of the fitted poles and residues in compare to the the original admittance of the $\frac{\lambda}{4}$ monopole antenna with respect to frequency is shown in Figure 3.6. As this figure shows the fitted poles and residues fit perfectly the original

admittance function.

Subsequently, using circuit synthesis theory and equations (3.5) and (3.6), an equivalent circuit model, with two complex conjugate pole, has been employed as the monopole antenna feed point impedance model. The calculated components values of each branch has been presented in Table 3.1

**Table 3.1:** Component values of the equivalent circuit model branches for the 8cm long wire $\frac{\lambda}{4}$ monopole antenna.

| | Resistance ($\Omega$) | Inductance(H) | Capacitance($\mu$F) |
|---|---|---|---|
| Branch 1 | $4.4576 \times 10^3$ | 0 | 0 |
| Branch 2 | 0 | 0 | $1.7284 \times 10^{-7}$ |
| Branch 3 | 17.0849 | $5.366 \times 10^{-8}$ | $1.073 \times 10^{-6}$ |
| Branch 4 | 24.879 | $5.704 \times 10^{-8}$ | $1.081 \times 10^{-7}$ |

The time domain simulation result is represented in Figure 3.7. Figure 3.7a shows the time domain result for 70 ns and Figure 3.8 shows the frequency domain results. As the figure demonstrates the center frequency is 918.1 MHz and the $-3$ dB band width is 9.3 MHz.

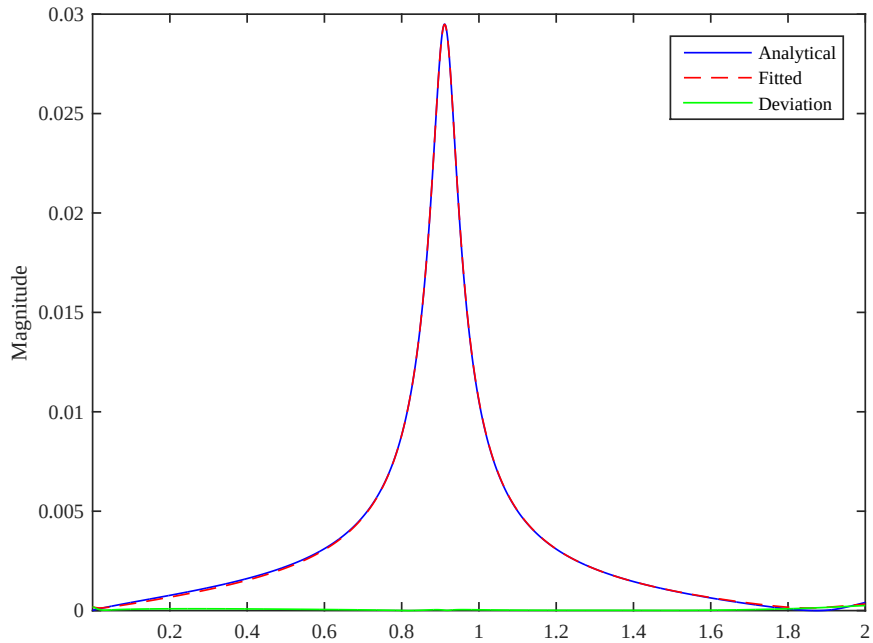


**(a)**

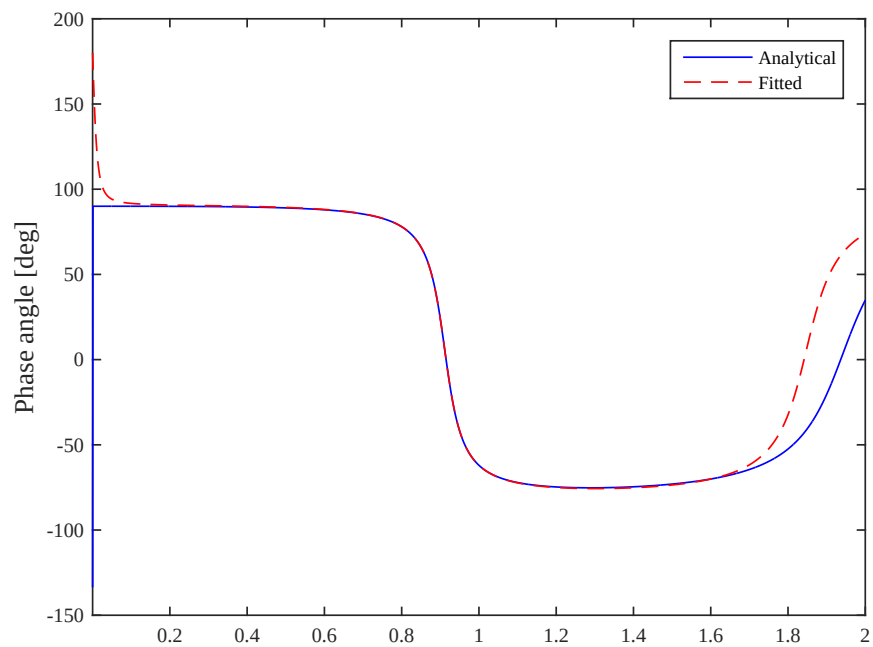


**(b)**

**Fig. 3.6:** The admittance of the fitted poles and residues compared to the original admittance of a $\frac{\lambda}{4}$ monopole antenna with respect to frequency (a) Magnitude (b) Phase.

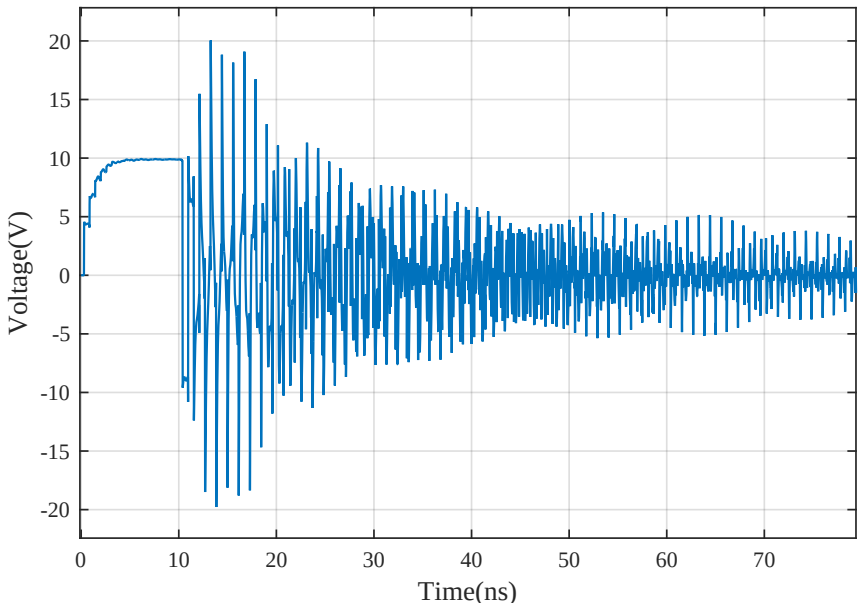


**(a)**

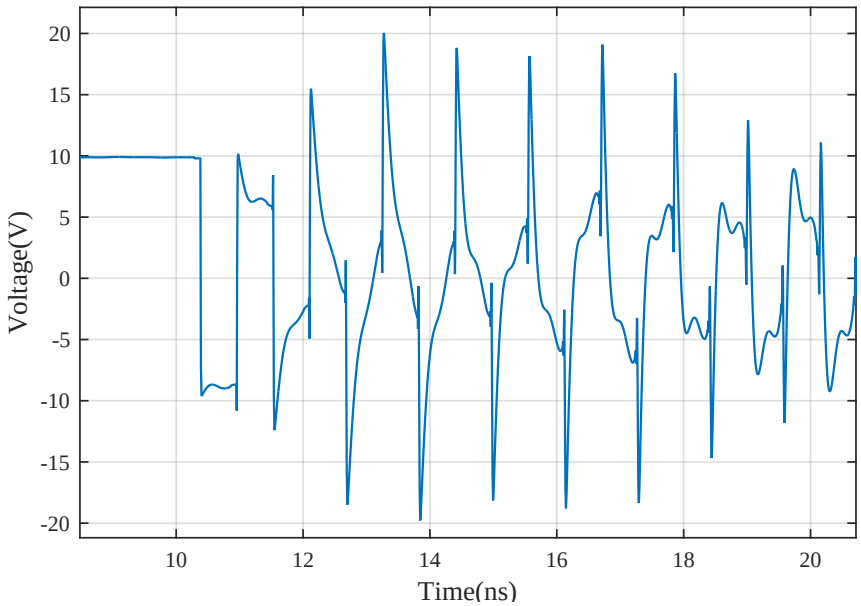


**(b)**

**Fig. 3.7:** Simulation result of a switched oscillator with resonance frequency of 915 MHz (a) Time domain result (b) Time domain result for the time interval of 5-20 ns

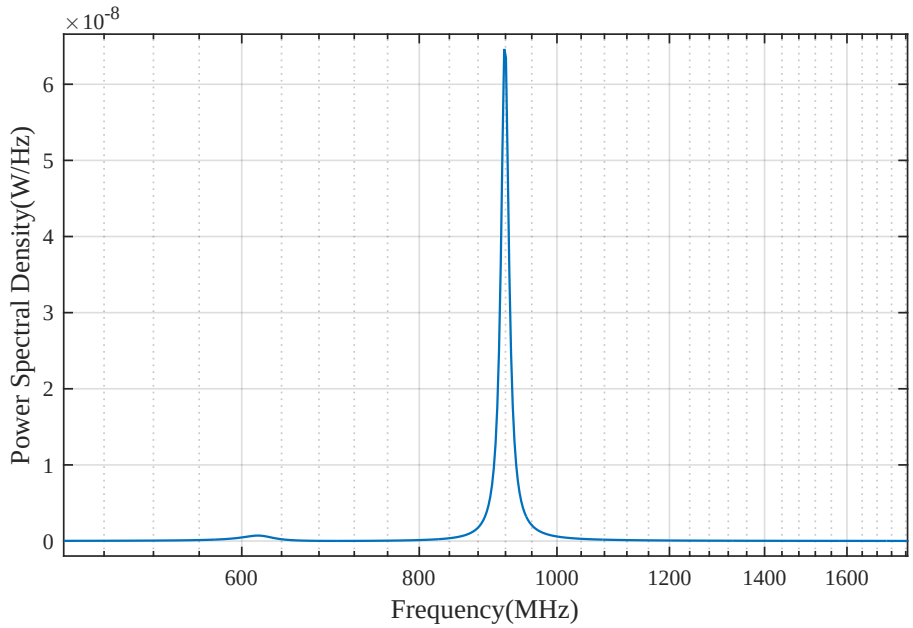


**Fig. 3.8:** Frequency domain simulation result of a switched oscillator with resonance frequency of 915 MHz.

### 3.3.1 Sensitivity Analysis

To identify the effects of any changes or fluctuations in determinative parameters on the switched oscillator output signal, some sensitivity tests have been performed. The determinative parameters includes:

1. Length of the transmission line
2. Characteristic impedance of the transmission line
3. Resonance frequency of the antenna
4. Switch transition time
5. Antenna feed point impedance

The result of these sensitivity tests are presented in the following:

- **The length of the transmission line:** In order to examine the impact of a change in the length of the transmission line on the switched oscillator output signal, three sets of simulations with ±10% difference in the transmission line length have been conducted. Figure 3.9 depicts the time domain and frequency domain result of the simulations in compare to initial simulation results. As expected, a change in the length of transmission line caused change in the center frequency of the switched oscillator. +10% increase in the transmission line length lead to +9.5% raise in the center frequency and −10% decrease in the transmission line length makes the center frequency lower by −9.4%. The bandwidth and amplitude of the signal stays almost the same.

- **The characteristic impedance of the transmission line:** In order to observe the influence of a variation in the characteristic impedance of the transmission line on the switched oscillator output signal, three sets of the simulations with ±30% modification in the characteristic impedance of the transmission line has been carried out. The result of the time domain and frequency domain simulations with three transmission line with 10Ω ,15Ω and 20Ω characteristic impedances are shown in figure 3.10. As this figure shows, by 30% reduction of the characteristic impedance of the transmission line, the amplitude of the power spectral density of the signal drops by 37.74% and by 30% increasing the characteristic impedance of the transmission line, the amplitude of the power spectral density of the signal rises by 105.13% which fits our expectation from theory that smaller characteristic impedance of the transmission line leads to higher reflection coefficient at antenna terminal and consequently higher amplitude of the signal.

- **The resonance frequency of the antenna:** With the purpose of identifying the impact of any fluctuations of antenna resonance frequency on the switched oscillator output signal, Three sets of simulations including three antennas with different resonance frequencies has been conducted. The resonance frequencies of the antennas varies by ±10% from 915 MHz. Figure 3.11 is illustrating the time domain and frequency domain results of the three simula-

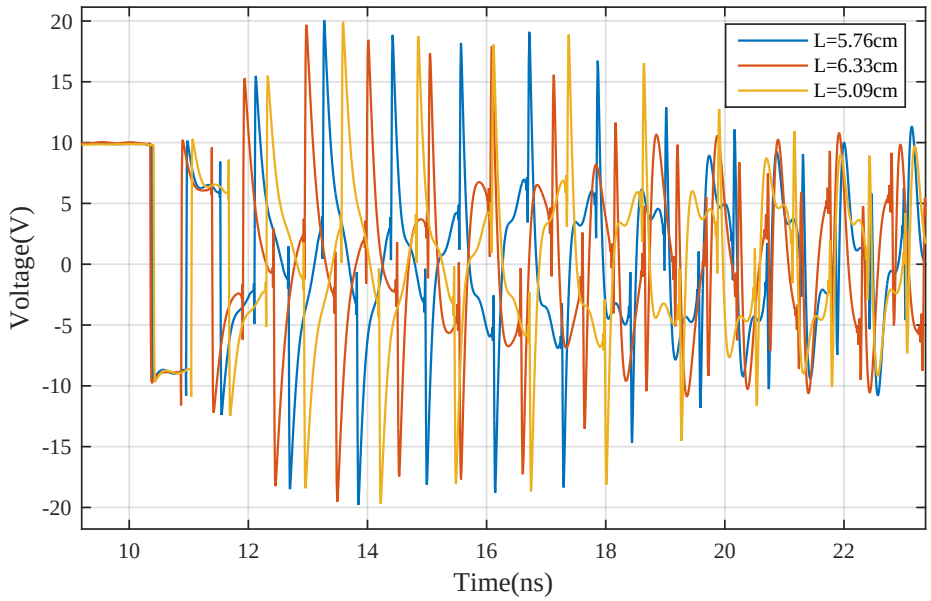


**(a)**

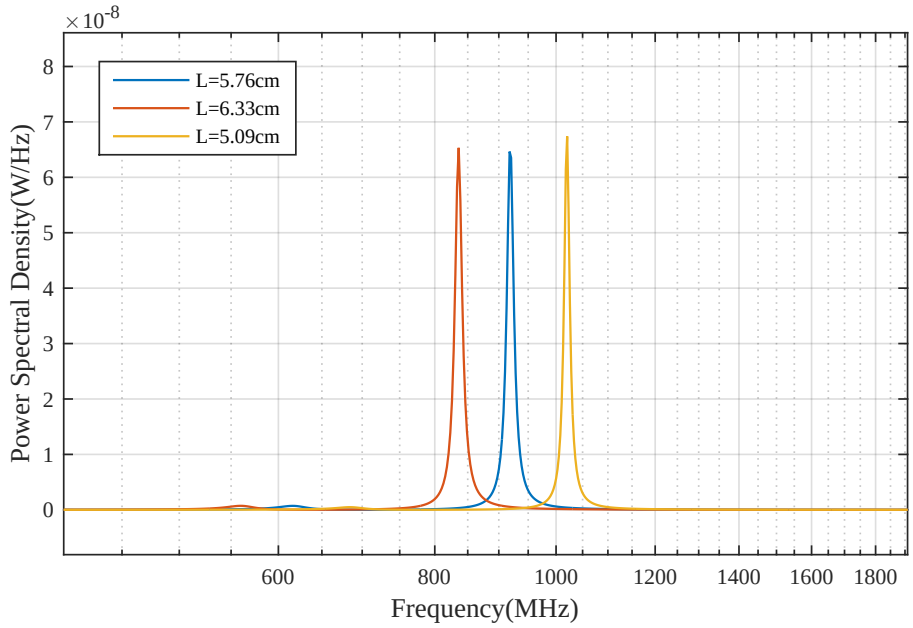


**(b)**

**Fig. 3.9:** Simulation results of a switched oscillator with different transmission line lengths (a) Time domain results (b) Frequency domain results.

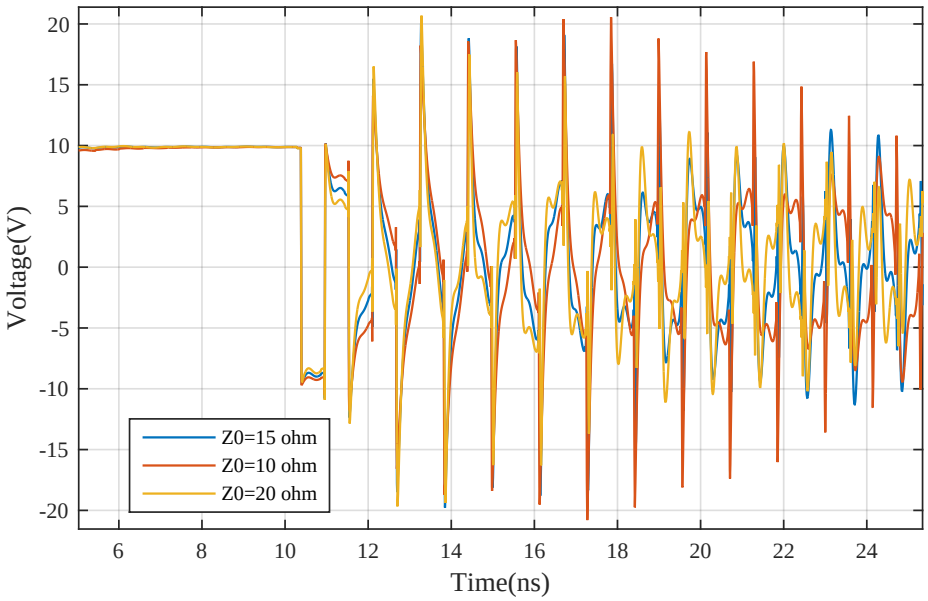


**(a)**

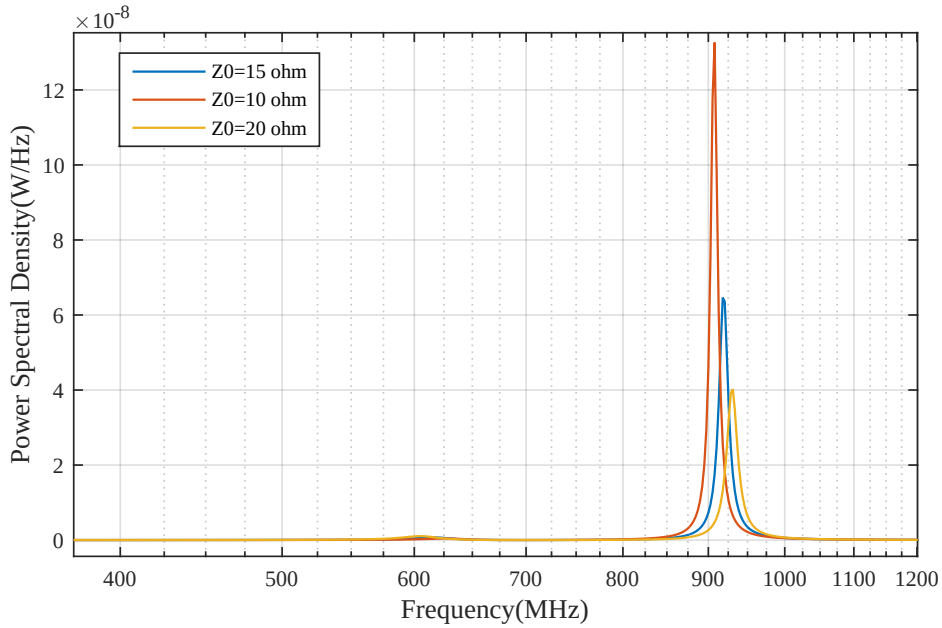


**(b)**

**Fig. 3.10:** Simulation results of a switched oscillator with different transmission line characteristic impedances (a) Time domain results (b) Frequency domain results.

tions. As the figure shows, variation of the resonance frequency of the antenna causes a slight change in the center frequency of the signal generated by the switched oscillator. Increasing the resonance frequency of the antenna by +10% leads to +2.8% raise in the center frequency of the signal generated by the switched oscillator and reducing the resonance frequency of the antenna by −10% leads to −1% decrease in the center frequency of the signal generated by the switched oscillator.

- **The switch transition time:** Regarding the effect of variation of the switch transition time on the switched oscillator output signal, three sets of simulations with three different switch transition times have been performed. The switches transition times are 100 ps, 1 ns and 2 ns. Figure 3.12 presents the time domain and the frequency domain of the three simulation results. As the figure shows, up to 1 ns transition time the impact of the variation of the switch transition time on the signal is negligible, however the transition times more than 1 ns causes fluctuation in the center frequency of the signal.

- **The antenna feed point impedance:** In order to identify the impact of variations of the antenna feed point impedance, two sets of simulations with two different antennas have been conducted. A dipole antenna and a monopole antenna were chosen for the simulations which the feed point impedance of dipole antenna is twice the feed point impedance of the monopole antenna. Figure 3.13 demonstrates the time domain and the frequency domain of the simulations results. The results show that the dipole antenna leads to higher amplitude of the pulses and consequently higher power spectral density of the signal than monopole antenna. That's because of the higher feed point impedance of the dipole antenna which makes the reflection coefficient larger and therefore the amplitude of the reflected signal toward the switch higher. By increasing the feed point impedance of the antenna by +100% the amplitude of the power spectral density of the signal rises by +302%. Using dipole antenna instead of monopole antenna also induced a slight change (−0.3%) in the center frequency.

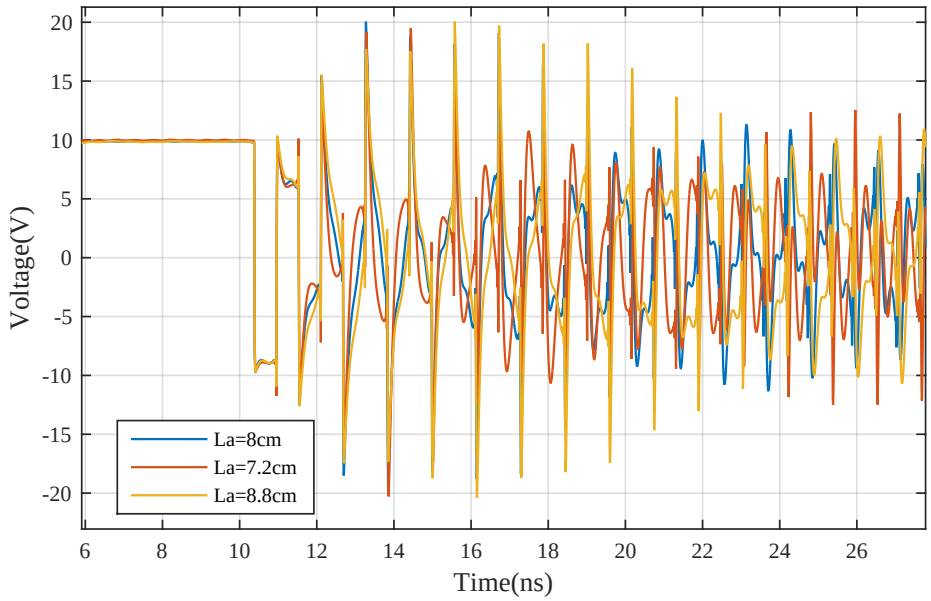


**(a)**

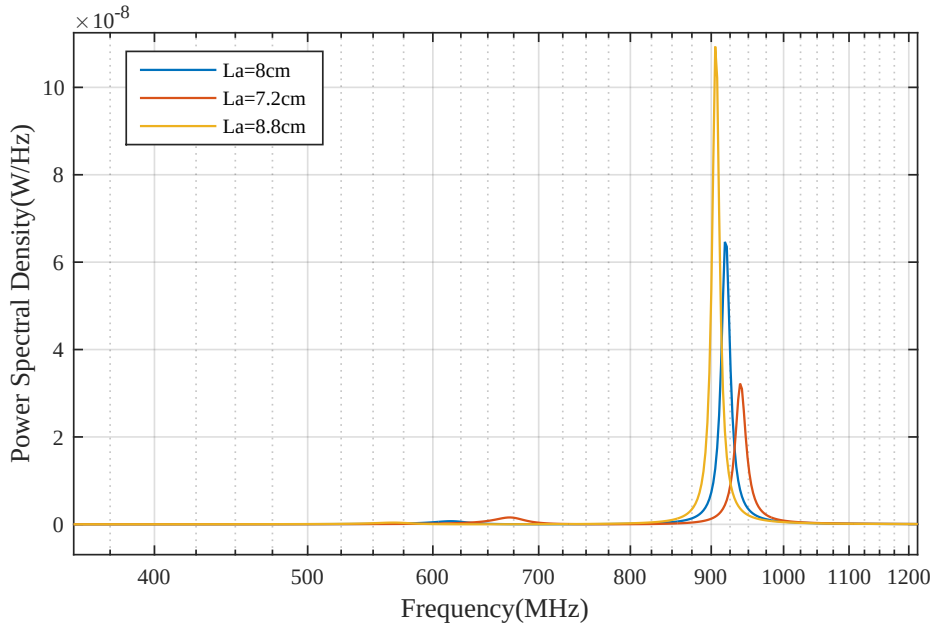


**(b)**

**Fig. 3.11:** Simulation results of a switched oscillator with different resonance frequency of the antennas (a) Time domain results (b) Frequency domain results.

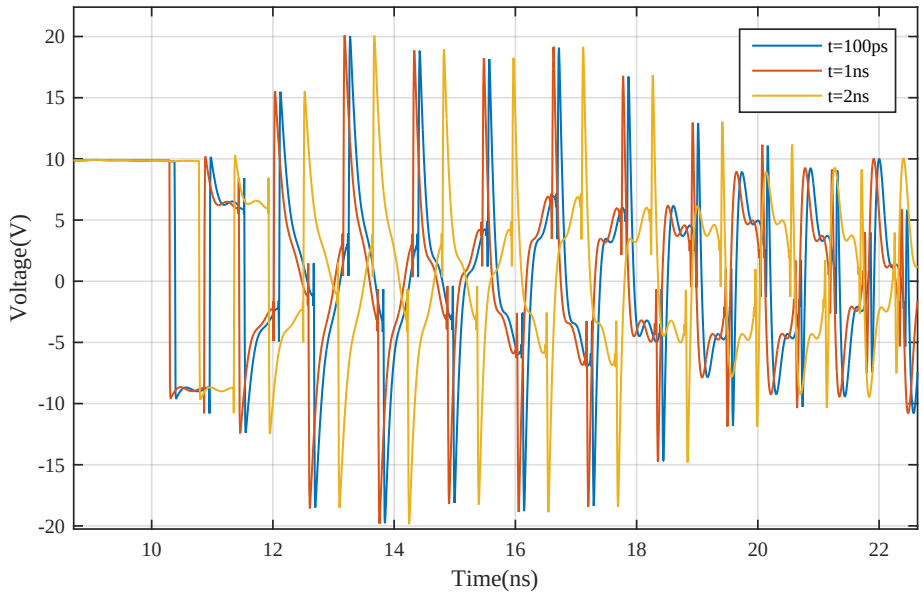


**(a)**

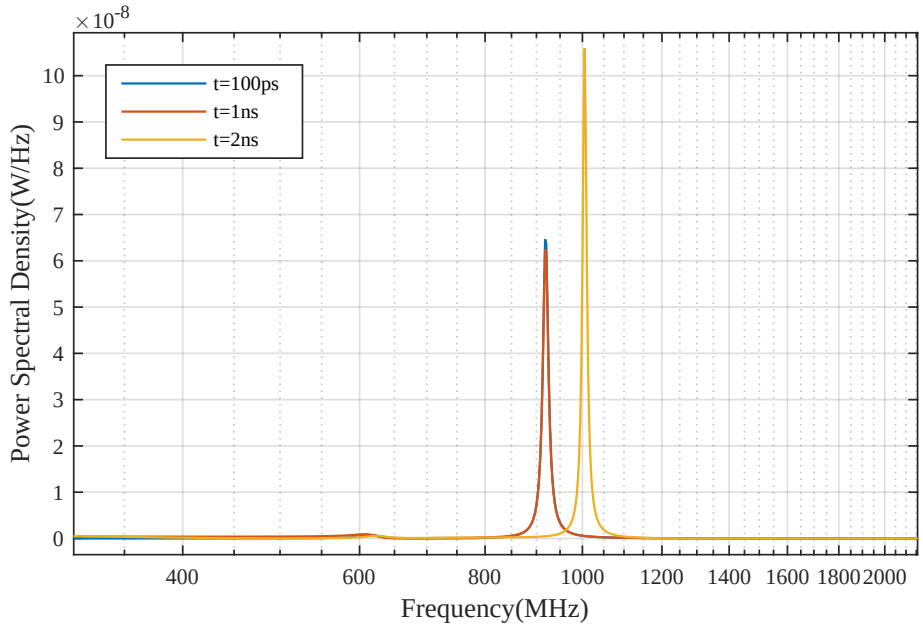


**(b)**

**Fig. 3.12:** Simulation results of a switched oscillator with different switch transition times (a) Time domain results (b) Frequency domain results.

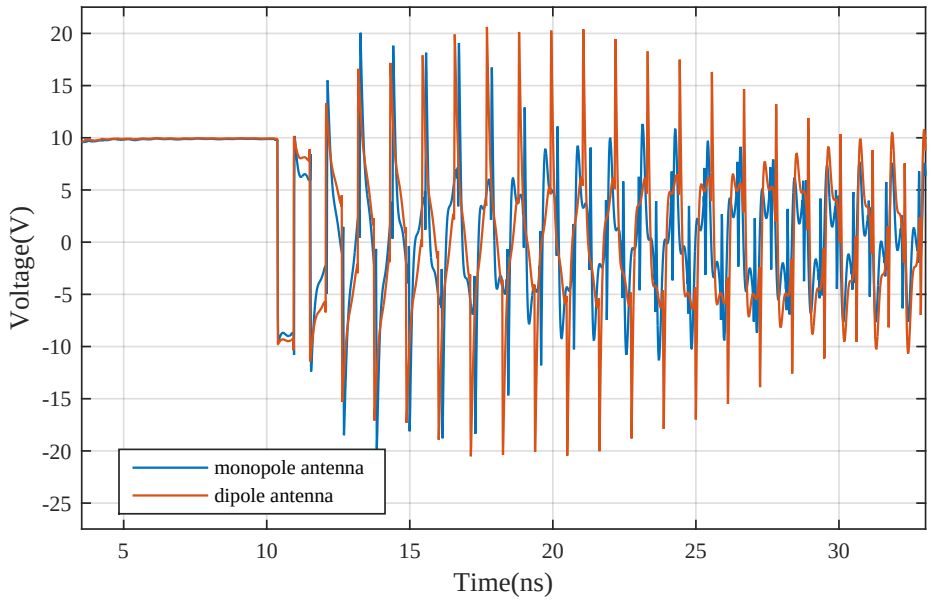


**(a)**

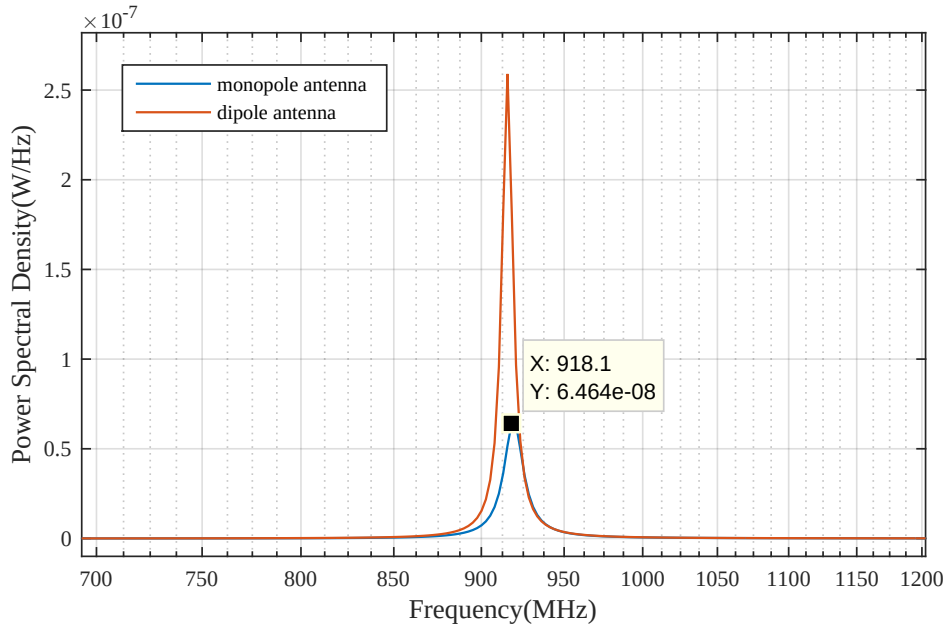


**(b)**

**Fig. 3.13:** Simulation results of a switched oscillator with different antenna feed point impedances (a) Time domain results (b) Frequency domain results.

## 3.4 Summary

In this chapter, the design procedure of the quarter wavelength switched oscillator in the ISM Band was presented. The design criteria were discussed in details. Different features which affect the design were studied. To optimize the design, a time domain simulation using PSCAD software has been conducted. Finally, a set of sensitivity analysis has been performed in the time domain to determine the determinative and limitative parameters in the switched oscillator design. The optimized designed quarter wavelength switched oscillator is capable of generating a decaying amplitude pulse with the center frequency of 915 MHz.

# Chapter 4

# Fabrication of Switched Oscillator

In this chapter, the fabrication of the proposed quarter wavelength switched oscillator is presented. Three fabricated prototype switched oscillators are demonstrated. Switched oscillator design is optimized to achieve the desired performance. Three prototype switched oscillator are fabricated with three different transmission lines and antennas. The first prototype has been fabricated using a coaxial cable as the transmission line and a monopole antenna. In the second prototype, a microstrip transmission line and a PCB monopole antenna have been employed, and the third prototype has been designed and fabricated using conductor backed coplanar waveguide (CBCPW) and a PCB monopole antenna. The fabrication procedure of each part of the three prototypes are presented in this chapter.

## 4.1 Fabrication Procedure

A switched oscillator is composed of a DC charging circuit to charge the transmission line, a fast switch to short circuit the transmission line and generate a fast transient through the line, a low impedance transmission line, and a higher impedance antenna to reflect back the fast transient and transmit the generated signal. A RF choke can be used as a high impedance in the working frequency of the switched oscillator to prevents effects of the DC charging circuit on the generated signal.

### 4.1.1 DC Charging Circuit

The circuit is a fly-back boost converter with a high voltage step-up transformer. A 555 timer and transistor Q1 drive the step up transformer. A diode-capacitor DC voltage doubler has been connected to the secondary coil of the transformer and a regulator has been used at the last stage of the circuit to regulate the output voltage at a stable value. The nominal input voltage is 9 V DC. The peak output voltage is approx. 7.5kV DC. The current capacity of the circuit is limited to less than 1mA by the small value of the capacitors in the doubling circuit[1].

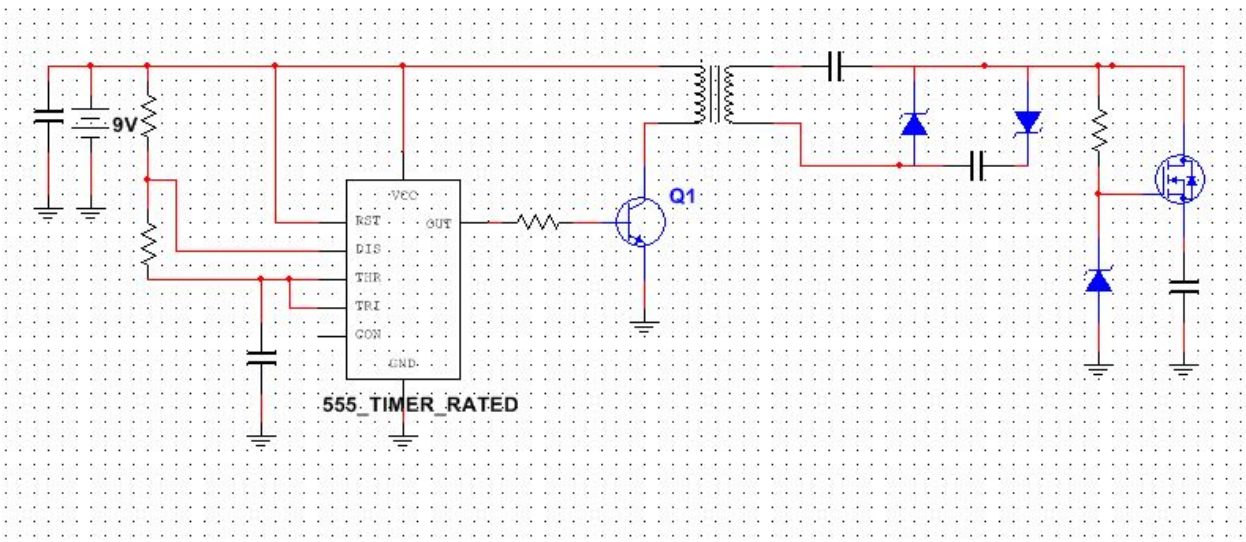


**Fig. 4.1:** DC charging citrcuit schematic consist of a fly-back boos converter with a high voltage step-up transformer. Input voltage is 9 V DC and the peak output voltage is around 7.5 kV DC.

### 4.1.2 Switch

As it was discussed in Section 3.2.2, the key features to choose a switch to incorporate into a switched oscillator are the transition time, which for 915 MHz switched oscillator needs to be less than 1 ns, the open state impedance which requires to be as high as possible, and the closed state impedance which has to be very small value. Furthermore, the switch has to be bilateral. It means

[1]This power supply was originally designed and provided by a third party.

that the switch needs to conduct equally well in both directions when it is on. Finding a switch with all these conditions was challenging. One not ideal but good enough choice would be a Gas Discharge Tube (GDT) switches.

A Gas Discharge Tube (GDT) consists of a tube (usually made of glass), with two or more electrodes inside the tube, that has been filled with a gas or gas mixture usually at a pressure less than the atmospheric pressure. Applying voltage to the electrodes ionizes the gas inside the tube. As the voltage applied across the electrodes reaches the "breakdown voltage", an avalanche process will initiate in the tube. The break down voltage depends on composition and pressure of the gas mixture and the distance of the electrodes [31]. To keep the GDT on, a "hold over voltage" needs to be across the electrodes. The GDT will switch back to high impedance state when there is not enough energy to keep the current flow. GDT switches have a very high insulation resistance (open state impedance), more than $10^{10}\Omega$, low closed state resistance (less than 10 $\Omega$) and very low capacitance (less that 1 pF). The transition time of GDT switches are not as fast as 1 ns. The transition time depends on the peak voltage over the GDT, The lower the peak voltage, the faster the GDT. The transition time also depends on the rate of the voltage change over GDT. Faster voltage chage results in lower transition time. Therefore, A GDT with the lowest breakdown voltage available is chosen and a fast rising pulse is used over the GDT switch.

The GDT has been used in this project is shown in figure 4.2 which is Littelfuse 2027 series with DC breakdown voltage of 90 V and DC hold over voltage of 52 V.

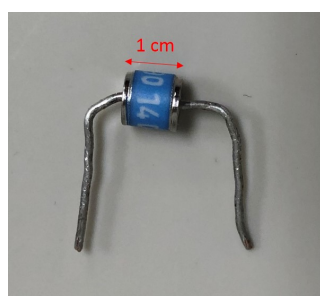


**Fig. 4.2:** The GDT Littelfuse 2027 series.

### 4.1.3 Transmission Line

In this research, three prototypes of the switched oscillator have been fabricated with three different transmission line: a coaxial cable, a microstrip transmission line and a Copalanar Waveguide(CPW).

- **Coaxial Cable:** In the first prototype, a SMA coaxial cable has been used as the transmission line in the switched oscillator design. Coaxial cables are low loss and the propagated signal attenuation is very low. Also because of the ground shielding around the center conductor, the outside interference and noise level is minimum. On the other hand, the shielding restricts the electric and magnetic fields to the dielectric layer between the conductors with little leakage and prevents interference with any nearby wave such as the electromagnetic wave propagated by the antenna that makes it a very good choice for the switched oscillator. The only problem is that the commercial SMA coaxial cables only come in 50 Ω and 75 Ω and the lower characteristic impedance is not available. In this prototype, Mini Circuit 141 Model Series coaxial cables has been employed. The 141 Model Series coaxial cables are wide band (DC-18 GHz) and low loss (0.07 dB at less than 2 GHz). Dielectric is low loss Polytetrafluoroethylene (PTFE) with a dielectric constant ($\varepsilon_r$) of 2.1 and the dissipation factor (tan $\delta$) of 0.0004. The characteristic impedance of the 141 Series coaxial cables is 50 Ω. The SMA coaxial cables come in the fixed length and are not available in the length needed for 915 MHz frequency which is a quarter of a wavelength at 915 MHz (5.65 cm). The length of the cable is 7.62 cm, therefore the expected frequency of the signal generated by the quarter wavelength switched oscillator based on (3.1) would be 679 MHz.

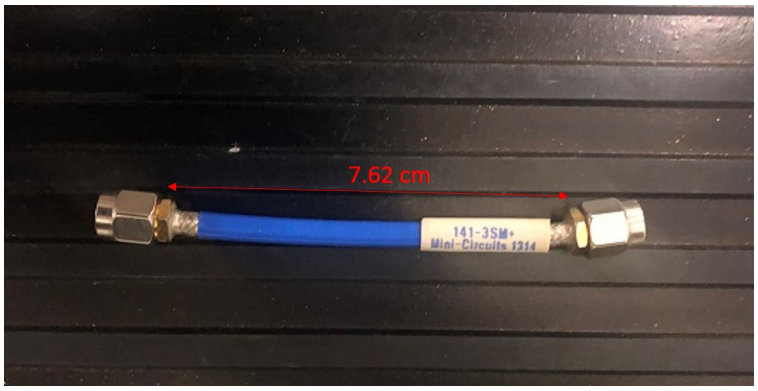


**Fig. 4.3:** Mini Circuit 141 Model Series coaxialwith the length of 7.62 cm.

- **Microstrip Line:** As it was discussed in Section 3.2.3 to fabricate the switched oscillator, a transmission line with 15 Ω characteristic impedance is desired. Since coaxial cable transmission line are not available in the characteristic impedances less than 50 Ω, in the second prototype, the coaxial cable transmission line has been replaced with a microstrip transmission line. The microstrip transmission line consists of a substrate layer with a conducting strip on the top and a conducting layer at the bottom as the ground layer. Figure 4.4 shows a microstrip transmission line configuration. Planar configuration of microstrip lines makes them uncomplicated to integrate with microwave devices and they all can be assembled on a compact PCB. Therefore, microstrip transmission lines are inexpensive and easy to fabricate.

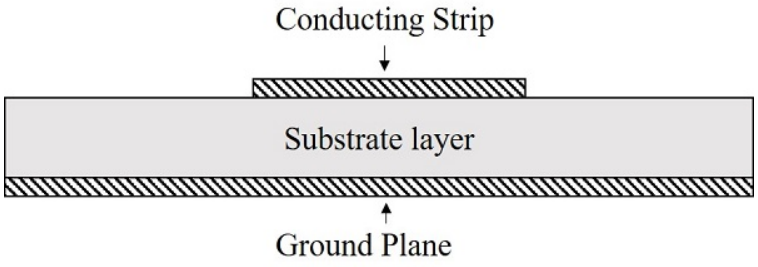


**Fig. 4.4:** Cross section view of a microstrip transmisson line configuration.

To design the microstrip transmission line, it is essential to keep in consideration that in a microstrip line electric and magnetic fields are propagating in two different mediums, air ($\varepsilon_r = 1$) and the substrate ($\varepsilon_r$), with two different dielectric constant. Consequently, phase velocity and propagation constant of the electromagnetic wave would vary in each medium. Therefore, an effective dielectric constant ($\varepsilon_e$) can be defined as an approximation of the equivalent dielectric constant of substrate-air medium. In other words, the effective dielectric constant ($\varepsilon_e$) can be consider as the dielectric constant of a homogeneous medium that replaces the inhomogeneous air-substrate medium. The effective dielectric constant ($\varepsilon_e$) can be calculated using 4.1 [32]

$$\varepsilon_e = \frac{\varepsilon_r + 1}{2} + \frac{\varepsilon_r - 1}{2} \frac{1}{\sqrt{1 + 12\frac{d}{W}}} \tag{4.1}$$

where $\varepsilon_r$ is the substrate dielectric constant, $d$ is the thickness of the substrate and $W$ is the width of the strip. Accordingly, phase velocity (c) and propagation constant (k) would be respectively, $\frac{c}{\sqrt{\varepsilon_e}}$ and $\frac{k}{\sqrt{\varepsilon_e}}$. Subsequently, the characteristic impedance of a microstrip transmission line can be calculated as [32]:

$$Z_0 = \begin{cases} \frac{60}{\sqrt{\varepsilon_e}} ln(\frac{8d}{W} + \frac{W}{4d}) & \text{for } \frac{W}{d} \leq 1 \\ \frac{120\pi}{\sqrt{\varepsilon_e}(\frac{W}{d} + 1.393 + 0.667 ln(\frac{W}{d} + 1.444))} & \text{for } \frac{W}{d} \geq 1 \end{cases} \tag{4.2}$$

To design the dimensions of the microstrip transmission line, for a given characteristic impedance $Z_0$, the ratio of $\frac{W}{d}$ can be calculated by [32].

$$\frac{W}{d} = \begin{cases} \frac{8e^A}{e^{2A} - 2} & \text{for } \frac{W}{d} < 2 \\ \frac{2}{\pi}[B - 1 - ln(2B - 1) + \frac{\varepsilon_r - 1}{2\varepsilon_r}(ln(B - 1) + 0.39 - \frac{0.61}{\varepsilon_r})] & \text{for } \frac{W}{d} > 2 \end{cases} \tag{4.3}$$

where

$$A = \frac{Z_0}{60}\sqrt{\frac{\varepsilon_r + 1}{2}} + \frac{\varepsilon_r - 1}{\varepsilon_r + 1}(0.23 + \frac{0.11}{\varepsilon_r})$$

$$B = \frac{377\pi}{2Z_0\sqrt{\varepsilon_r}}.$$

In this project RT/duroid 5870 laminate by Rogers Corporation has been used as the substrate of the microstrip transmission line. RT/duroid 5870 laminate is a glass microfiber reinforced PTFE composite which has been manufactured explicitly for stripline and microstrip applications. The dielectric constant of RT/duroid 5870 laminate is 2.33 and it is uniform and constant over a wide frequency range. Low dissipation factor (loss tangent between $0.0005 - 0.0012$) of this laminate results in very low dielectric loss. Thickness of the substrate is 0.787 mm and the strip and ground layer are composed of 17 $\mu$m electro-deposited copper foil.

To acquire a 15 $\Omega$ characteristic impedance for the designated microstrip transmission line, from (4.3), the ratio of $\frac{W}{d}$ has been found and a width of 10.94 mm has been chosen for the strip. The frequency and the substrate dielectric constant determine the length of the microstrip line to be 55.1 mm. Ground plane width needs to be more that 3W to perform as an infinite ground plane. The ground plane employed in this thesis is 55.1 mm long and 100 mm wide. The designed microstrip line has been simulated using Comsol multiphysics to find the exact value of the characteristic impedance of the microstrip line and other characteristic of the microstrip transmission line. The results of the simulation are presented in Table 4.1 and figure 4.5.

**Table 4.1:** Simulation result of microstrip transmission line parameter at 915 MHz.

| | |
|---|---|
| Characteristic Impedance ($\Omega$) | $15.011 - j0.021$ |
| Capacitance (F/m) | $3.63 \times 10^{-10}$ |
| Shunt Conductance (S/m) | $1.31 \times 10^{-6}$ |
| Distributed Inductance (H/m) | $8.18 \times 10^{-8}$ |
| Distributed Resistance ($\Omega$/m) | 1.3477 |
| Propagation Constant (1/m) | $0.044 + j31.35$ |

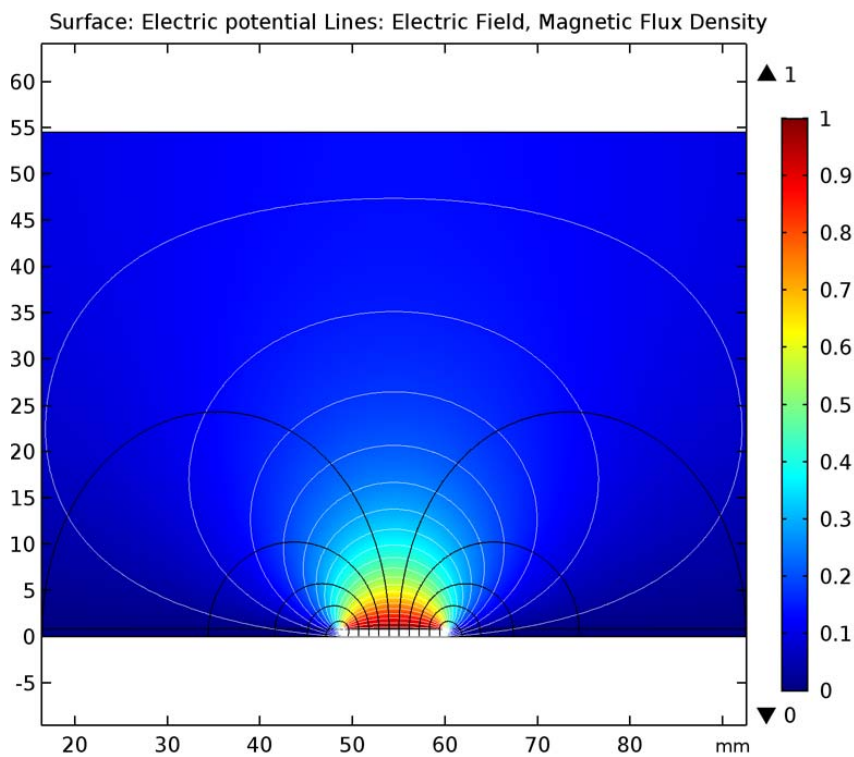


**Fig. 4.5:** Electric field and magnetic field line of a microstrip transmission line with 15 $\Omega$ characteristic impedance

Figure 4.6 shows the fabricated microstrip line.

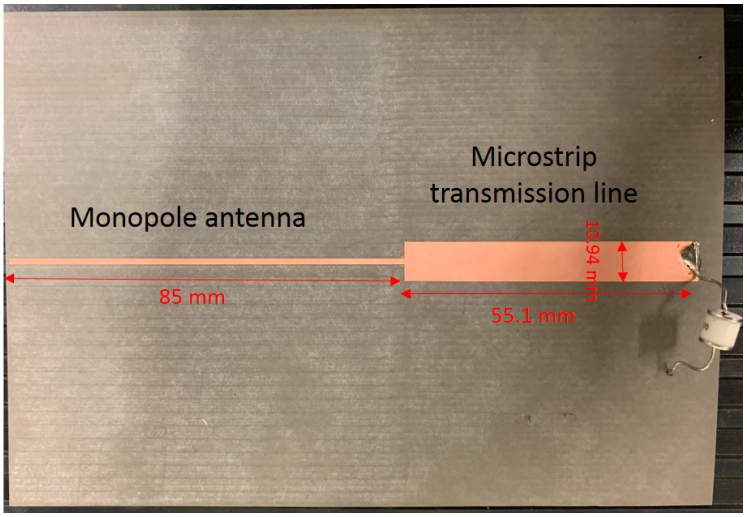


**Fig. 4.6:** Microstrip transmission line with 55mm long and 10.94 mm wide strip connected to a printed monopole antenna.

- **Conductor Backed Coplanar Waveguide (CBCPW):** In the third prototype a Conductor Backed coplanar waveguide (CBCPW) has been employed as a substitute for the microstrip line. Like microstrip line, the CBCPW consists of a dielectric substrate layer, a conductor strip on top and ground layer at bottom of the dielectric substrate layer. The difference between CBCPW and microstrip line is that in a CBCPW, there are also two ground plane on top of the substrate, on each side of the conductor strip. The two top layer grounds are connected to the bottom layer ground by means of vias. Figure 4.7 shows a conductor backed coplanar waveguide configuration.

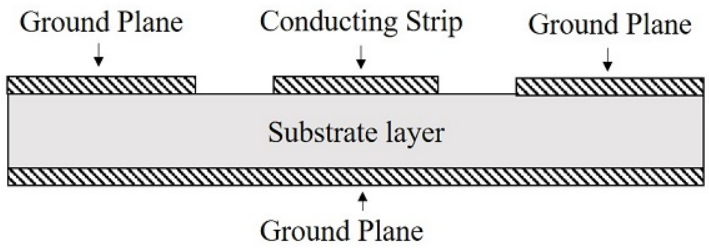


**Fig. 4.7:** Cross section view of a CBCPW transmisson line configuration.

The ground planes on top layer of CBCPW facilitates surface mounting of passive and active components. Also, because of the ground planes on top layer, CBCPW is less prone to interferencee and has more isolation than microstrip transmission line [33]. Since the amount of the electric and magnetic fields in the air is higher compared to a microstrip line, the effective dielectric constant of a CBCPW is up to 15% lower than the effective dielectric constant of a microstrip line. The effective dielectric constant and characteristic impedance of the CBCPW can be calculated using [34]

$$\varepsilon_{\mathrm{e}} = \frac{1 + \varepsilon_{\mathrm{r}} \dfrac{K(k')}{K(k)} \dfrac{K(k_3)}{K(k_3')}}{1 + \dfrac{K(k')}{K(k)} \dfrac{K(k_3)}{K(k_3')}} \tag{4.4}$$

$$Z_0 = \frac{60\pi}{\sqrt{\varepsilon_{\mathrm{eff}}} \dfrac{K(k)}{K(k')} + \dfrac{K(k_3)}{K(k_3')}} \tag{4.5}$$

where

$$k = \frac{w}{w + 2S},$$

$$k_3 = \frac{\tanh(\pi w/4d)}{\tanh(\pi[w+2S]/4d)},$$

$$k' = \sqrt{1.0 - k^2},$$

$$k_3' = \sqrt{1.0 - k_3^2}$$

and $w$ is the width of the conductor strip, $S$ is the gap between the conductor strip and each top layer ground, $d$ is the dielectric substrate thickness and $K(k)$ is the complete elliptic integral of the first kind. For the case where, the gap between the conductor strip and top layer grounds is more than 2 times the substrate layer thickness($S > 2d$), CBCWP operates very similar to microstrip transmission line and the characteristic impedance of both transmission lines with the same substrate and the same conductor strip width would be the same. [35]

To design the CBCPW, an online calculator [36] has been used. This online calculator, that uses (4.4) and (4.5) calculates the values of characteristic impedance and electrical length of the CBCPW transmission line for given values of width of conductor strip, the gap between the conductor strip and top layer ground planes, substrate thickness, dielectric constant of substrate, length of traces and frequency. The online calculator also can evaluate the width of conductor strip and the gap between the conductor strip and top layer ground planes for a given value of characteristic impedance.

The designed CBCPW line has been simulated using Comsol multiphysics to find the exact value of the characteristic impedance of the CBCPW line. The result of the simulation are presented in Table 4.2 and figure 4.8.

**Table 4.2:** Simulation result of CBCPW transmission line parameter at 915 MHz.

| | |
|---|---|
| Characteristic Impedance ($\Omega$) | $15.751 - j0.018$ |
| Capacitance (F/m) | $4.17 \times 10^{-10}$ |
| Shunt Conductance (S/m) | $1.52 \times 10^{-6}$ |
| Distributed Inductance (H/m) | $7.18 \times 10^{-8}$ |
| Distributed Resistance ($\Omega$/m) | 1.1755 |
| Propagation Constant (1/m) | $0.044 + j31.49$ |

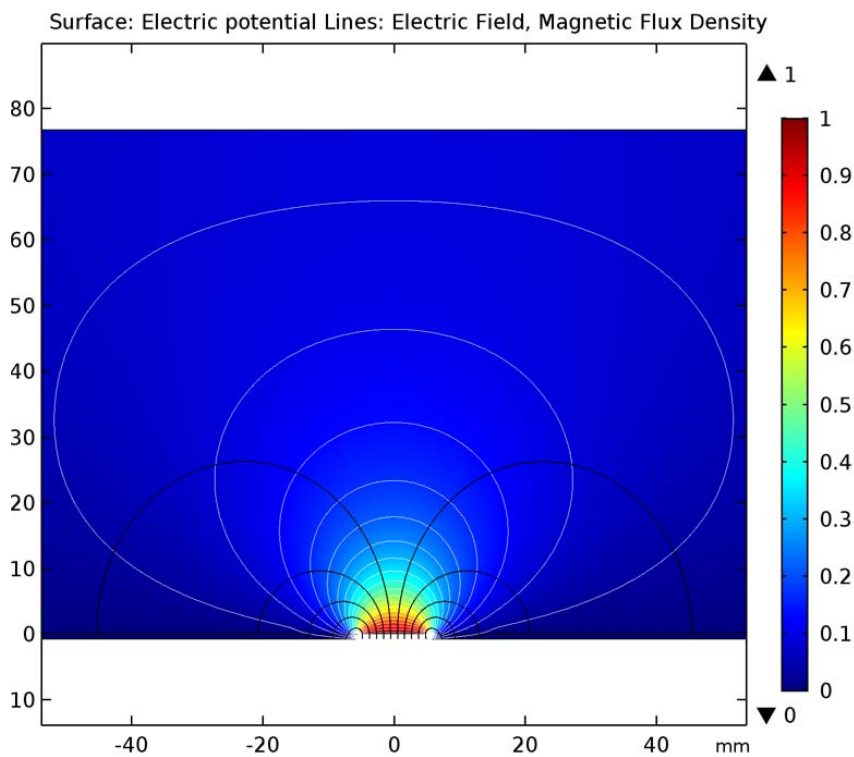


**Fig. 4.8:** Electric field and magnetic field line of a CBCPW with 15 $\Omega$ characteristic impedance

To fabricate the CBCPW with a 15 Ω characteristic impedance at 915 MHz the substrate RT/duroid 5870 laminate by Rogers Corporation with 2.33 dielectric constant and 0.787 mm thickness has been employed. The width of the conductor strip is 10.96 mm and the gap between the conductor strip and top layer ground planes is 10mm which is bigger than twice of the dielectric thickness(0.787 mm). The length of the transmission line is 55 mm and the width of each top layer ground plane is 59.5 mm. The width of the bottom layer ground is 150 mm. Figure 4.9 shows the fabricated CBCPW transmission line.

Additionally, in the third prototype, all different component of the switched oscillator has been soldered on the transmission line board and all the wires kept at the minimum length possible to reduce noise and any power loss in the connections.

### 4.1.4 Antenna

The switched oscillator impulse generator designed to interrogate a number of electric field sensors in different locations. Therefore, a linear polarization antenna with wide directivity is desired. Monopole antenna is linearly polarized and its pattern covers all the perpendicular planes and it is a suitable choice for this application.

- **Monopole Antenna:** In the first prototype, a quarter wavelength monopole antenna has been employed in the switched oscillator configuration. The quarter wavelength monopole antenna length with the first resonance frequency of 679 MHz is 11 cm but because of relatively high characteristic impedance of the coaxial cable transmission line (50 Ω) and relatively low input impedance of the monopole antenna at its first resonance frequency (34 Ω), a monopole antenna with 8 cm ($\lambda/4$) long wire on a ground plane with first resonance frequency of 915 MHz is chosen which has been shown in figure 4.10.

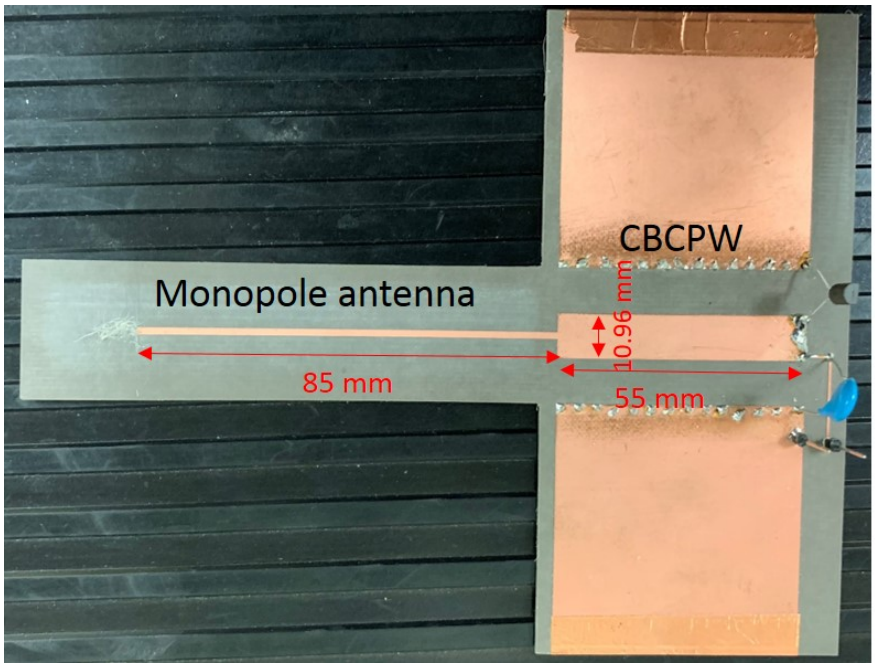


**(a)**

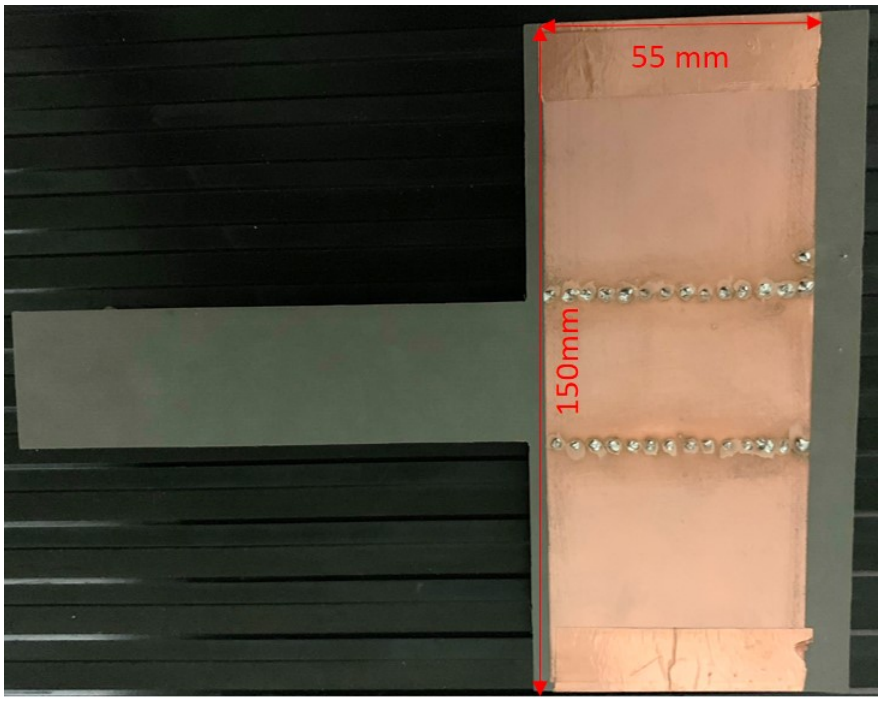


**(b)**

**Fig. 4.9:** Fabricated CBCPW transmisson line a) Front side. A 55 mm long and 10.96 mm wide strip connected to a printed monopole antenna, (b) Back side. the bottom layer ground, 55 mm long and 150 mm wide.

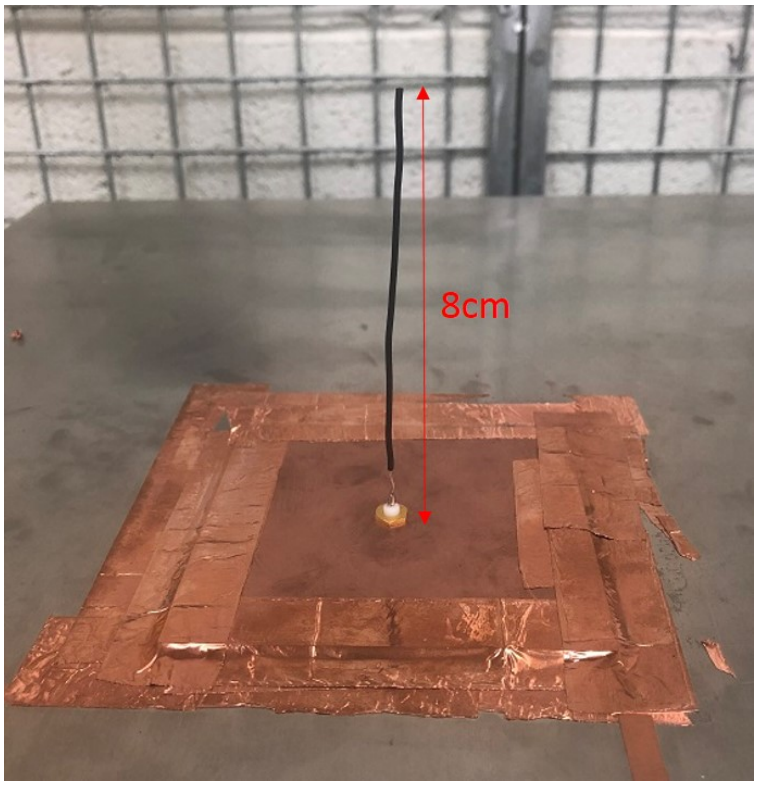


**Fig. 4.10:** Quarter wavelength monopole antenna (11 cm long wire).

- **Printed Monopole Antenna:** In the second and third prototypes, the aim was to make a planar switched oscillator on a printed circuit board. Therefor, a printed monopole antenna has been designed and fabricated for the switched oscillator. Furthermore, the printed monopole antenna can be fabricated on the same substrate of both microstrip and CBCPW transmission line and the antenna connects directly to the transmission line that avoids any loss or unwanted reflection. The fabricated printed monopole antenna has been shown in Figure 4.9 and 4.6. The width of the strip is 1.5 mm and the length of strip is 85 mm [37].

### 4.1.5 RF Choke

In the switched oscillator topology, a DC source charges the transmission line and subsequently the switch short-circuits the transmission line. With the purpose of blocking any impact of the DC source on the waveform generated by the switched oscillator, a RF choke has been employed. The RF choke is an inductor with a very low impedance at DC and high impedance at its self-resonance frequencies. Therefore it passes DC signals and blocks signals at its self-resonance frequency. Self-resonance frequency of a Rf choke is the frequency which the parasitic capacitance of the RF choke resonates with the inductance of the RF choke resulting in an extremely high impedance. [38] The RF choke B78108E with the inductance of 100 nH and self resonance frequency of 700 MHz has been used in the first prototype switched oscillator. The RF choke LQW15CA from Murata Electronics North America with the inductance of 560 nH and self resonance frequency of 900 MHz has been employed in the fabricated planar switched oscillators.

## 4.2 Simulation Results of the CBCPW Switched Oscillator

A time-domain simulation using finite element method by Comsol Multiphysics has been run on the proposed CBCPW switched oscillator. Figure 4.11 shows the geometry of the CBCPW switched oscillator. A 150 $\times$ 150 cm RT/duroid 5870 laminate with 2.33 dielectric constant and 0.787 mm thickness has been employed as the substrate. Bottom layer ground is 150 cm wide and 55 mm long. There are two top layer grounds, 59.5 mm wide and 55 mm long each. The conductor strip is a 10.96 mm wide and 55 mm long and there is 10 mm gap between the conductor strip and each top layer ground. A printed monopole antenna with a width of 1.5 mm and a length of 85 mm is connected to the conductor strip.

In a switched oscillator, after charging the transmission line, the switch closes and short-circuits the transmission line. To simulate the effect of switch on the circuit, a pulse has been applied to the input port of the transmission line, such that, at first, the voltage is zero then the charging

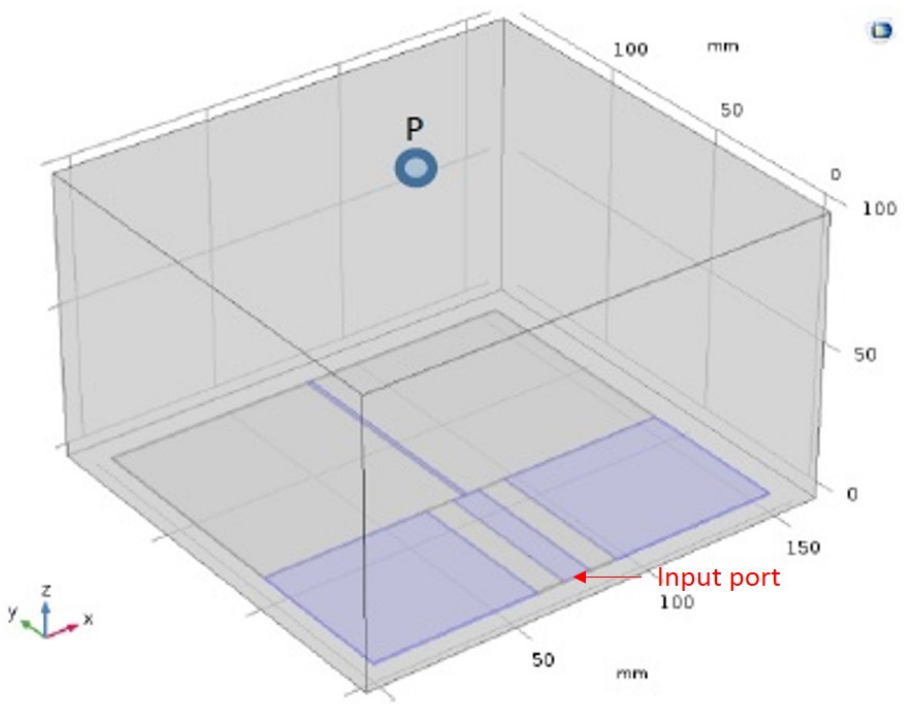


**Fig. 4.11:** Geometry of the proposed CBCPW transmission line simulated using Comsol Multiphysics.

circuit charges the transmission line and after that switch closes and vltage goes to zero again. The transmission line charges to 1 V in 25 ns then the input changes to zero and short circuits the transmission line.

Electric field radiated by the CBCPW Switched oscillator at point P at a distance of 10 cm, 50 cm and 100 cm has been evaluated. The absolute magnitude of the electric field at point P has been plotted in fig 4.12 , 4.13 and 4.14. At a distance of 10 cm, the maximum of radiated electric field is 2.3 $V/m$. Radiated electric field in near field region is proportional to the inverse-square of the distance ($1/r^2$) and by increasing the distance, the maximum of radiated electric field deceases by order of 2. As these figure shows, the electric field at 50 cm distance is about 1/25 times of the electric field at 10 cm and the electric field at 100 cm is about 1/100 times of the electric field at 10 cm. The radiated electric field lasts for 10 ns.

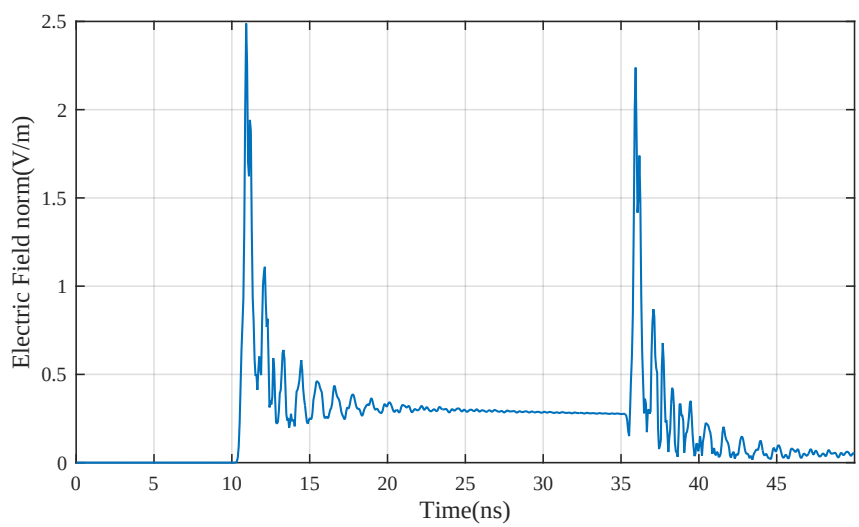


**Fig. 4.12:** Radiated electric field of poroposed CBCWP switched oscillator at 10 cm.

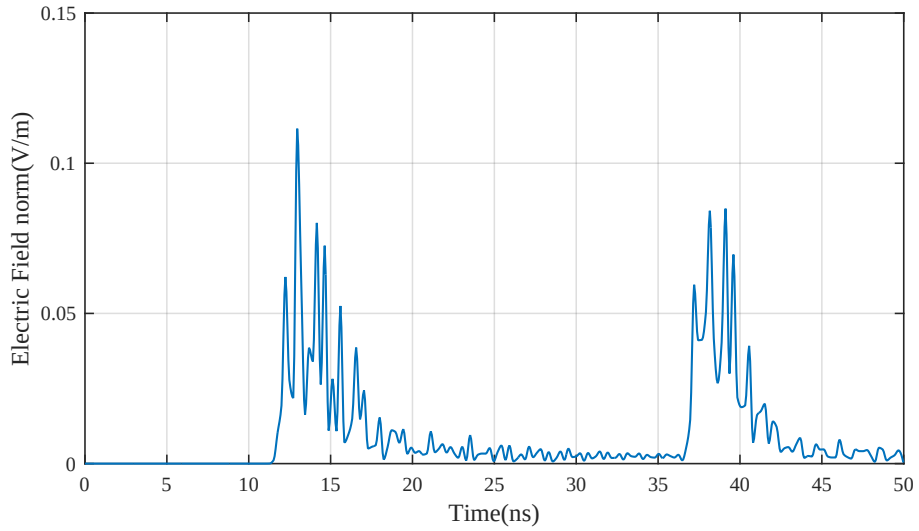


**Fig. 4.13:** Radiated electric field of poroposed CBCWP switched oscillator at 50 cm.

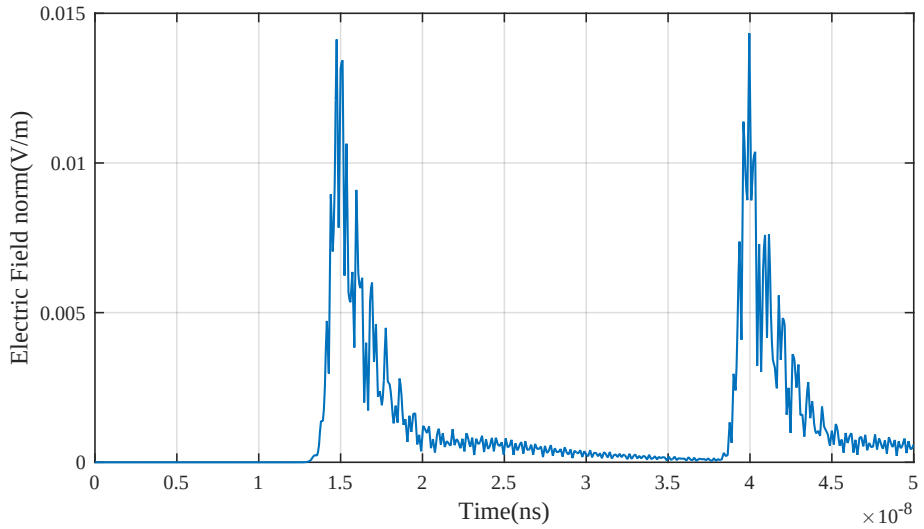


**Fig. 4.14:** Radiated electric field of poroposed CBCWP switched oscillator at 100 cm distance.

## 4.3 Summary

Fabrication procedure of the switched oscillator has been presented. Three switched oscillator prototypes have been designed, fabricated, and assembled. The first prototype consists of a DC charging circuit, a gas discharged tube as the switch, a coaxial cable transmission line and a monopole antenna. This prototype operates at 680 MHz. The second prototype is a planar switched oscillator. Therefore, the coaxial cable in the first prototype has been replaced by a microstrip transmission line and a printed monopole antenna has been used instead of monopole antenna. The third prototype is very similar to the second prototype, only a CBCPW is used as the transmission line. The second and third prototypes have been designed to perform at 915 MHz.

# Chapter 5

# Switched Oscillator Test and Characterization

In this chapter, testing and characterization of the fabricated switched oscillator are discussed. The experimental setup is described and the performance of the three fabricated switched oscillator is experimentally tested and evaluated. The experimental data is provided to test and justify the theoretical model and simulation results presented in previous chapters.

## 5.1 Switched Oscillator Experimental Setup

In the previous chapter, three prototypes for the switched oscillator have been introduced. The experimental setup to test and characterize the fabricated switched oscillators has been described in figure 5.1a and 5.1b. The first prototype switched oscillator consists of a coaxial cable transmission line, a monopole antenna, a gas discharge tube as the switch, an RF choke and the DC charging circuit described in Section 4.1.1. Figure 5.2 shows the charging circuit. The signal generated by the first switched oscillator has been measured by a commercial D-dot AD-S30 electric field sensor made by Prodyn. D-dot is a very precise high frequency electric field sensor that measures the rate of change of the electric displacement over time in a wide range of frequency. The bandwidth of AD-S30 is more than 1 GHz, its rise-time is less than 0.35 ns and its output range is ±4 KV. picture

of D-dot AD-S30 has been presented in figure 5.3. The distance between the monopole antenna and the sensor was 30 cm. Both monopole antenna and D-dot sensor were at the same height from the ground. The second and third prototype switched oscillators are planar. The transmission line in the second prototype is a microstrip antenna and the antenna is a printed monopole antenna. In the third prototype a CBCPW has been employed instead of a microstrip transmission line. A $3 \times 3$ cm parallel plate capacitive sensor with a 2 mm air dielectric has been used to measure the planar switched oscillators. The parallel plate capacitive sensor has been shown in figure 5.4. The parallel plate capacitive sensor was placed 10 cm above the printed monopole antenna. In both setup the probe is placed within the near-field region of the monopole antennas.

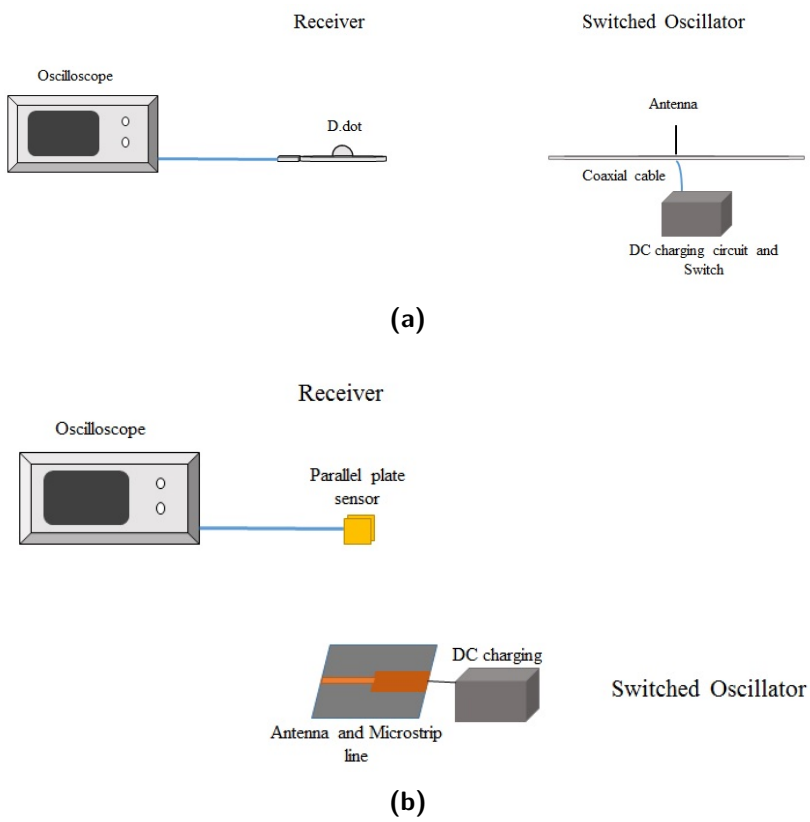


**Fig. 5.1:** (a)Experimental setup for the switched oscillator including coaxial cable and monopole antenna. (b) Experimental setup for the switched oscillator including microstrip/CBCPW transmission line and printed monopole antenna.

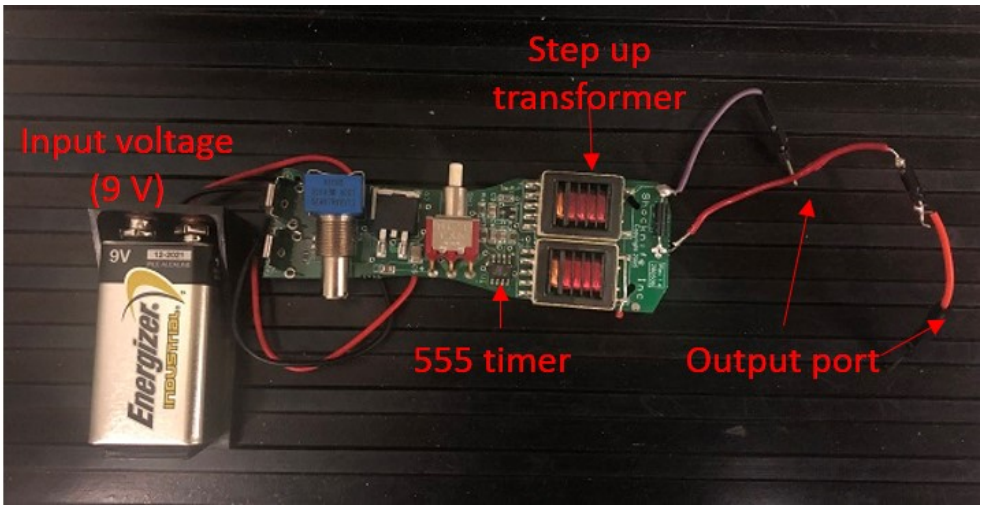


**Fig. 5.2:** DC charging citrcuit

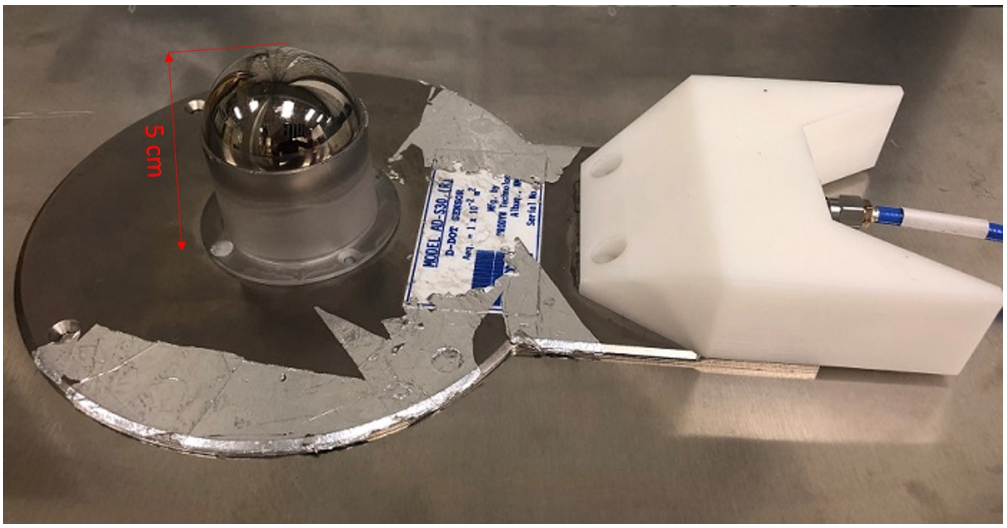


**Fig. 5.3:** D-dot AD-S30 sensor employed to measure signal for the switched oscillator including coaxial cable and monopole antenna.

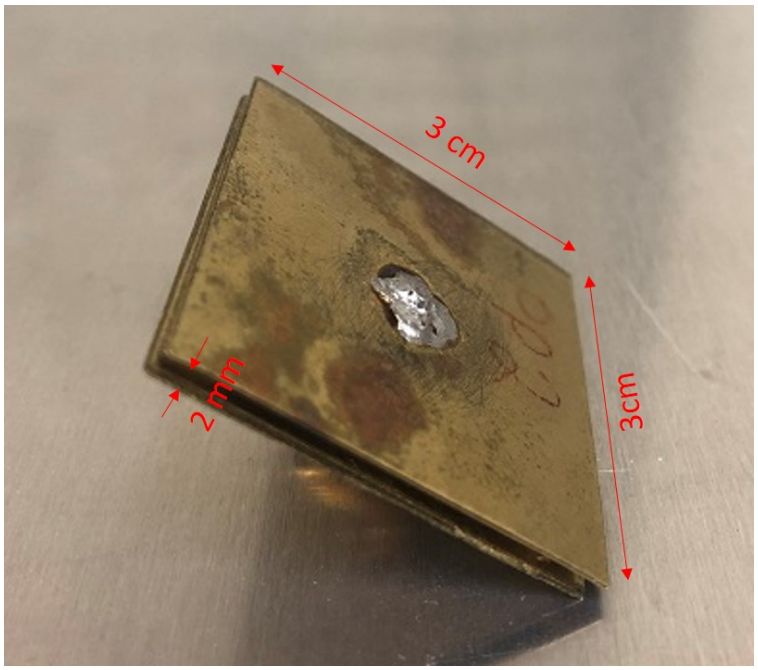


**Fig. 5.4:** D-dot AD-S30 sensor employed to measure signal for the switched oscillator including coaxial cable and monopole antenna.

## 5.2 Switched Oscillator Measurement Result

A number of tests have been conducted on the three fabricated switched oscillator by charging the transmission line through the DC charging circuit. After the GDT switch closes, the generated signal propagates toward the D-dot sensor (for coaxial cable switched oscillator) or Capacitive sensor (for microstrip switched oscillator and CBCWP switched oscillator). The measurement of the switched oscillator signal has been performed by connecting the D-dot sensor or capacitive sensor to the DSO9254A oscilloscope by Agilent Technologies. The measurement result of the coaxial cable switched oscillator and CBCPW switched oscillator has been reported in the following. The microstrip switched oscillator did not provide legitimate results. It could be because of the higher loss in microstrip transmission line. Therefore, the very low signal to noise ratio, made the

generated signal indistinguishable.

### 5.2.1 Result of the Switched Oscillator with Coaxial Cable Transmission Line

Figure 5.5 presents the electric field of the coaxial cable switched oscillator measured with the d-dot sensor. The measured peak amplitude of the signal is 0.17 V/m. Most of the energy of the signal contains in the time interval of 3 nsec to 13 nsec that is because of the small mismatch between coaxial cable transmission line characteristic impedance and monopole antenna input impedance.

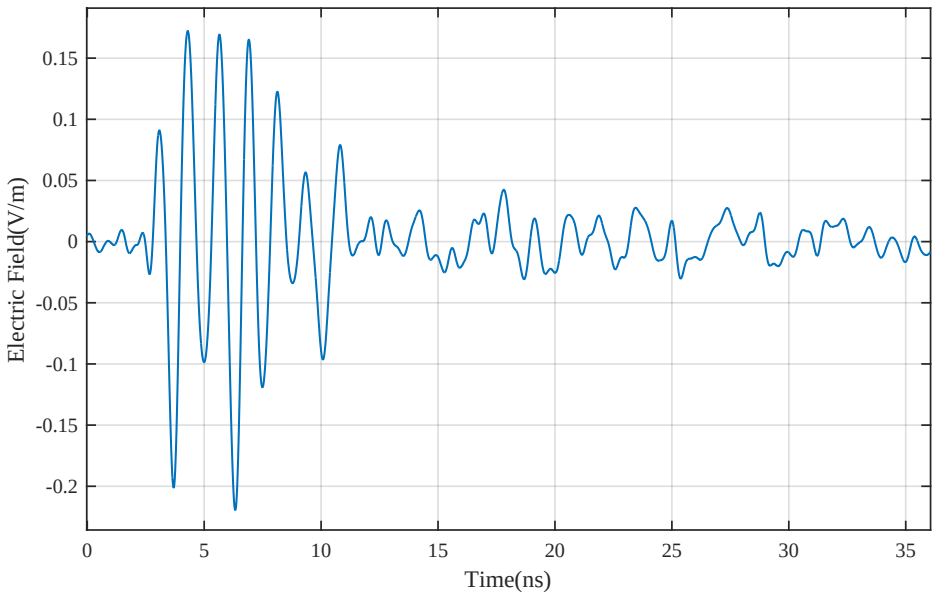


**Fig. 5.5:** Measurement result of the switched oscillator with coaxial cable transmission line and monopole antenna.

### 5.2.2 Measurement Result of the Third Switched Oscillator with CBCPW Transmission Line

Figure 5.6 shows the electric field measurement result of the CBCPW switched oscillator, measured by the parallel plate capacitive sensor. The measured peak amplitude of the signal is 0.04 V/m which is a lot less than the peak amplitude signal of the coaxial cable switched oscillator. The higher loss of a CBCPW transmission line than a coaxial cable transmission line is an explanation for the lower peak amplitude of the CBCPW switched oscillator signal. On the other hand, sensitivity of the parallel plate capacitive sensor is less than the D-dot electric field sensor and it could be another reason for the lower peak amplitude. The duration of the signal is about 80 nsec which is more than the duration of coaxial cable switched oscillator and it is due to higher mismatch between CBCPW transmission line characteristic impedance (15 Ω) and printed monopole antenna input impedance (34 Ω).

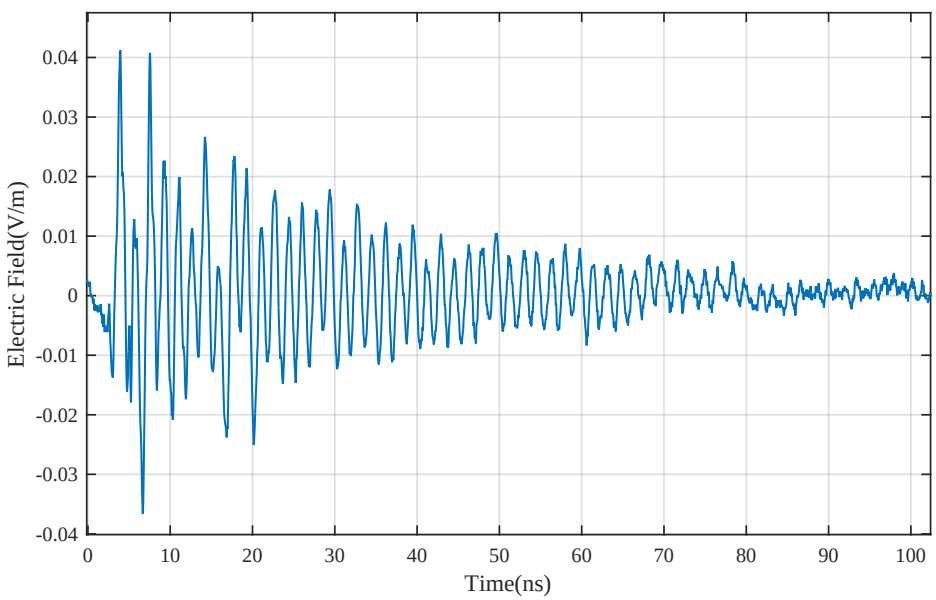


**Fig. 5.6:** Measurement result of the switched oscillator with CBCPW transmission line and printed monopole antenna.

## 5.3 Switched Oscillator Performance Evaluation

To evaluate the performance of the fabricated switched oscillators in the frequency domain, the power spectral density of the measured signal has been calculated using Matlab by

$$PSD = \frac{1}{F_s N} | \sum_{i=1}^{N} x_n e^{-j\omega_n / F_s} |^2 \tag{5.1}$$

where $F_s$ is the sampling frequency, $N$ is the number of samples, $x_n$ is the Electric field signal, and $\omega_n$ is angular frequency

### 5.3.1 Frequency Analysis of the Switched Oscillator with Coaxial Cable Transmission Line

Figure 5.7 represents the power spectral density of the measurement results of the coaxial cable switched oscillator. As the figure depicts, the power spectral density has two peaks, very close to each other. The first peak, happens at 715 MHz and the second peak appears at 798 MHz. Both peaks are higher than the expected frequency which was 679 MHz (see Section 4.1.3). The reason might be the difference between the resonance frequency of the quarter wavelength coaxial cable transmission line and the resonance frequency of the monopole antenna. Adjusting the length of the monopole antenna and subsequently the first resonance frequency of the antenna results in changes in the peak frequencies.

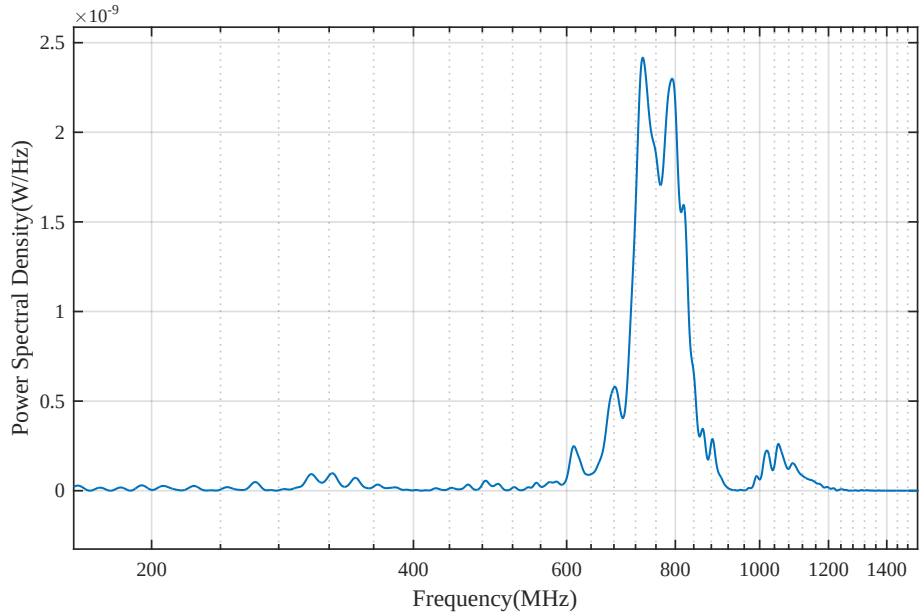


**Fig. 5.7:** Power spectrum of the result of the switched oscillator with coaxial cable transmission line and monopole antenna.

### 5.3.2 Frequency Analysis of the Switched Oscillator with CBCPW Transmission Line

The power spectral density of the measurement results of the CBCPW switched oscillator has been demonstrated in figure 5.8. Due to the perfect match between the resonance frequency of the quarter wavelength CBCPW transmission line and the first resonance frequency of the printed monopole antenna, power spectral density has only one peak. The resonance frequency of the CBCPW switched oscillator is 598 MHz which is not what we expect (915 MHz). The reason could be the wires that connect the DC charging circuit to the transmission line. The length of the wires add to the length of the transmission line, resulting in decreasing the resonance frequency. In this

prototype the wires are in the shortest length possible, but still they are about 1 cm long and moved the resonance frequency to 598 MHz.

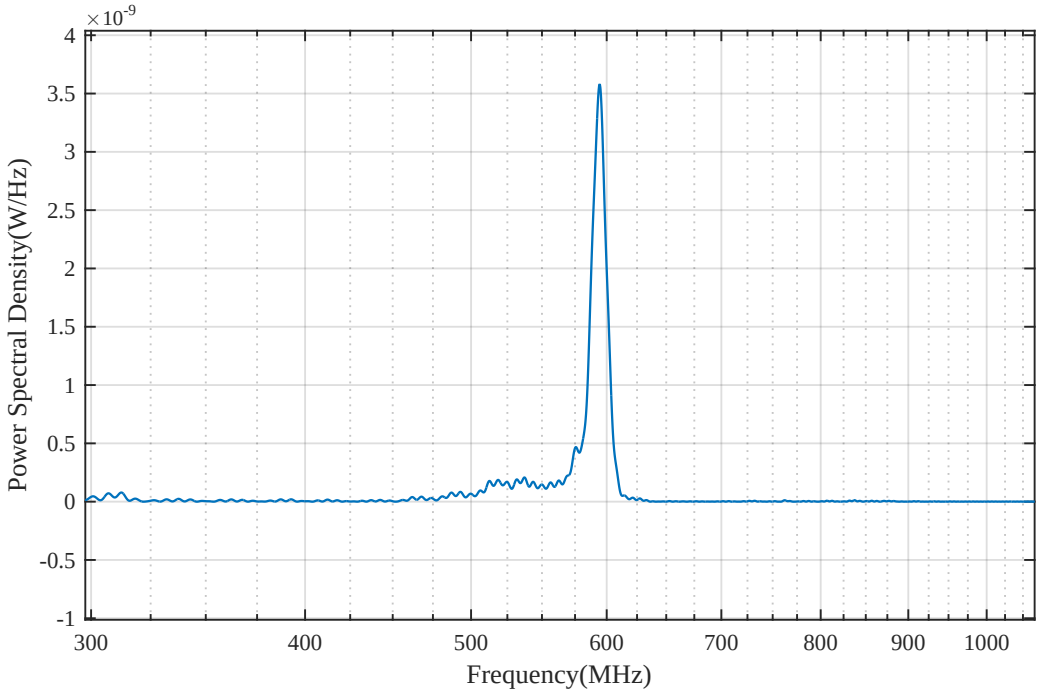


**Fig. 5.8:** Power spectrum of the result of the switched oscillator with CBCPW transmission line and printed monopole antenna.

## 5.4 Summary

Testing and evaluation of the coaxial cable switched oscillator and CBCPW switched oscillator were presented in this chapter. The experimental setup for each switched oscillator prototype has been demonstrated in detail and the measurement results of each prototype has been presented, interpreted and compared to each other. The frequency domain performance of the fabricated switched

oscillator has been calculated using power spectral density and evaluated. Switched oscillator with coaxial cable transmission line resonances at 717 MHz and the switched oscillator with CBCPW transmission line resonances at 598 MHz.

# Chapter 6

# Conclusions

In this thesis project, the design, simulation, fabrication, and assessment of a wireless integrated impulse generator have been presented. A switched oscillator has been fabricated as the impulse generator. The switched oscillator is composed of a transmission line with low characteristic impedance terminated to an antenna with a higher feed point impedance at one end and a shorting switch at the other end. A DC source charges the transmission line and then the switch operates and short circuits the transmission line and generates a transient wave. The transient wave propagates toward the antenna and the mismatch between transmission line and antenna makes a major portion of the wave reflect back toward the switch with reverse amplitude. Another reflection happens at the switch and subsequently a series of positive and negative pulses with decreasing amplitude will be generated at the antenna terminal and propagates by the pulse radiating antenna.

The switched oscillator impulse generator was designed to operate at ISM band of 902 MHz to 928 MHz. The proposed switched oscillator impulse generator is applicable as part of the remote interrogation system of a passive, wireless electric field sensor, designed to measure the AC electric field in the vicinity of the high voltage apparatus.

The proposed switched oscillator is a novel impulse generator that simplifies the configuration of the electric field sensor interrogation system and improves the center frequency and bandwidth

control. Measurement results captured using the designed prototype switched oscillator, have proven the applicability of the switched oscillator as a compact wireless pulse generator.

## 6.1 Future Work

In this thesis, the measurement results show that the proposed switched oscillator is operable to generate impulse waves and transmit it. The proposed switched oscillator impulse generator can be improved to enhance the accuracy of the center frequency and bandwidth of the generated signal and decrease the limiting errors and losses occurred during the fabrication process.

In this section, further studies to improve the proposed switched oscillator impulse generator are suggested. The possible applications to evaluate the proposed sensor are presented as well.

- The proposed switched oscillator potentially has up to 100 MHz bandwidth. The speed of the switch shorting the transmission line determines the bandwidth and center frequency accuracy. In order to get accurate bandwidth and center frequency high speed bidirectional switch is needed.

- The mismatch between transmission line characteristic impedance and antenna feed point impedance determines the amplitude and subsequently the duration of generated pulses. Therefore, designing a high feed point antenna would improve the performance of the proposed switched oscillator amplitude and duration. A high feed point impedance patch antenna would be a feasible choice.

- To increase the mismatch between transmission line characteristic impedance and antenna feed point impedance an impedance mismatch network could be employed. It has the same idea of an impedance matching network but instead of matching the impedances increases the impedance mismatch. A mismatch transformer is an example of the mismatch network.

- Designing a lower characteristic impedance transmission line is another way of increasing the mismatch between transmission line and antenna.

- The DC charging circuit used as the source for the proposed switched oscillator, induces noise in the generated signal. In order to reduce of eliminate this noise, some improvement in the DC charging circuit would be helpful.

- To eliminate the noises caused by the DC charging circuit a RF choke has been employed. But, the shielding of the RF choke seems to not be enough. Providing a better shielding could improve the switched oscillator performance.

- The wires connecting the DC charging circuit are a source of inaccuracy of the proposed switched oscillator center frequency. Fabricating the DC charging circuit on the same PCB substrate of switched oscillator and using as short as possible wires would eliminate this source of error.

# References


[1] J. Casazza, J. Casazza, and F. Delea, *Understanding electric power systems: an overview of the technology and the marketplace.* John Wiley & Sons, 2003, vol. 13.

[2] V. C. Gungor, B. Lu, and G. P. Hancke, "Opportunities and challenges of wireless sensor networks in smart grid," *IEEE Transactions on Industrial Electronics*, vol. 57, no. 10, pp. 3557–3564, 2010.

[3] A. Baki, "Continuous monitoring of smart grid devices through multi protocol label switching," *IEEE Transactions on Smart Grid*, vol. 5, no. 3, pp. 1210–1215, 2014.

[4] Q. Tan, T. Luo, T. Wei, J. Liu, L. Lin, and J. Xiong, "A wireless passive pressure and temperature sensor via a dual lc resonant circuit in harsh environments," *Journal of Microelectromechanical Systems*, vol. 26, no. 2, pp. 351–356, April 2017.

[5] J. Yao, S. Tjuatja, and H. Huang, "Real-time vibratory strain sensing using passive wireless antenna sensor," *IEEE Sensors Journal*, vol. 15, no. 8, pp. 4338–4345, Aug 2015.

[6] V. Viikari, J. Song, and H. Seppa, "Passive wireless sensor platform utilizing a mechanical resonator," *IEEE Sensors Journal*, vol. 13, no. 4, pp. 1180–1186, April 2013.

[7] S. Bhadra, D. S. Y. Tan, D. J. Thomson, M. S. Freund, and G. E. Bridges, "A wireless passive sensor for temperature compensated remote ph monitoring," *IEEE Sensors Journal*, vol. 13, no. 6, pp. 2428–2436, June 2013.

[8] M. Yazdani, D. J. Thomson, and B. Kordi, "Passive wireless sensor for measuring ac electric field in the vicinity of high-voltage apparatus," *IEEE Transactions on Industrial Electronics*, vol. 63, no. 7, pp. 4432–4441, July 2016.

[9] S.Mohammadzamani and B.Kordi, "Wireless integrated switched oscillator impulse generator with application in wireless passive electric field sensors," *World Academy of Science, Engineering and Technology International Journal of Physical and Mathematical Sciences*, vol. 13, no. 4, April 2019.

[10] D. M. Pozar, *Microwave engineering.* John Wiley & Sons, 2009.

[11] C. E. Baum, "Switched oscillators," *Circuit and Electromagnetic System Design Note*, vol. 45, no. 10, 2000.

[12] J. F. Vega Stavro, "Analytical methods for the study and design of integrated switched oscillators and antennas for mesoband radiation," *EPFL*, 2013.

[13] M. Armanious, J. S. Tyo, M. C. Skipper, M. D. Abdalla, W. D. Prather, and G. Gruen, "Electrostatic field management and electrodynamic modeling of switched quarter-wave oscillators," *IEEE Transactions on Dielectrics and Electrical Insulation*, vol. 18, no. 4, 2011.

[14] W. D. Prather, C. E. Baum, R. J. Torres, F. Sabath, and D. Nitsch, "Survey of worldwide high-power wideband capabilities," *IEEE Transactions on Electromagnetic Compatibility*, vol. 46, no. 3, pp. 335–344, Aug 2004.

[15] C. E. Baum, "Differential switched oscillators and associated antennas," *Circuit and Electromagnetic System Design Note*, vol. 457, no. 10, 2001.

[16] ——, "Differential switched oscillators and associated antennas. part 2," in *2004 Second International Workshop Ultrawideband and Ultrashort Impulse Signals (IEEE Cat. No.04EX925)*, Sep. 2004, pp. 13–15.

[17] ——, "The lumped-element switched oscillator," *Circuit and Electromagnetic System Design Note*, 2008.

[18] ——, "More antennas for the switched oscillator," *Circuit and Electromagnetic System Design Note*, 2004.

[19] ——, "Variations on the switched-oscillator theme," in *2010 URSI International Symposium on Electromagnetic Theory*, Aug 2010, pp. 1–4.

[20] M. Armanious, J. S. Tyo, M. C. Skipper, M. D. Abdalla, W. D. Prather, and J. E. Lawrance, "Interaction between geometric parameters and output waveforms in high-power quarter-wave oscillators," *IEEE Transactions on Plasma Science*, vol. 38, no. 5, pp. 1124–1131, 2010.

[21] F. Vega, F. Rachidi, N. Mora, B. Daout, N. Peña, and F. Roman, "A method for the analysis and design of switched oscillators using chain parameters," Tech. Rep., 2013.

[22] D. V. Giri, F. M. Tesche, M. D. Abdalla, M. C. Skipper, and M. Nyffeler, "Switched oscillators and their integration into helical antennas," *IEEE Transactions on Plasma Science*, vol. 38, no. 6, pp. 1411–1426, June 2010.

[23] Y. Wang, D. Chen, J. Zhang, S. Cao, D. Li, and C. Liu, "Investigation of a compact coaxially fed switched oscillator," *Review of Scientific Instruments*, vol. 84, no. 9, p. 094705, 2013.

[24] A. Budak, *Passive and active network analysis and synthesis.* Waveland PressInc, 1991.

[25] G. Antonini, "Spice equivalent circuits of frequency-domain responses," *IEEE Transactions on Electromagnetic Compatibility*, vol. 45, no. 3, pp. 502–512, Aug 2003.

[26] A. Ramirez, "Vector fitting-based calculation of frequency-dependent network equivalents by frequency partitioning and model-order reduction," *IEEE Transactions on Power Delivery*, vol. 24, no. 1, pp. 410–415, Jan 2009.

[27] H. S. Alharbi, "Power transformer transient modeling using frequency response analysis," *M.Sc. thesis, University of Manitoba*, 2014.

[28] C. a. Balanis, *Antenna Theory: Analysis Design, Third Edition, by Constantine A. Balanis*, 2005.

[29] B. Gustavsen and A. Semlyen, "Rational approximation of frequency domain responses by vector fitting," *IEEE Transactions on Power Delivery*, vol. 14, no. 3, pp. 1052–1061, July 1999.

[30] B. Gustavsen, "Computer code for rational approximation of frequency dependent admittance matrices," *IEEE Transactions on Power Delivery*, vol. 17, no. 4, pp. 1093–1098, Oct 2002.

[31] J. D. Cobine, "The development of gas discharge tubes," *Proceedings of the IRE*, vol. 50, no. 5, pp. 970–978, May 1962.

[32] D. M. Pozar, *Microwave engineering.* John Wiley & Sons, 2009.

[33] B. C. Wadell, *Transmission line design handbook.* Artech House, 1991.

[34] R. N. Simons, *Coplanar waveguide circuits, components, and systems.* John Wiley & Sons, 2004, vol. 165.

[35] J. Coonrod and B. Rautio, "Comparing microstrip and cpw performance," *Microwave Journal*, vol. 55, no. 7, pp. 74–86, 2012.

[36] D. McMahill. Coplanar waveguide analysis/synthesis calculator. [Online]. Available: http://wcalc.sourceforge.net/cgi-bin/coplanar.cgi

[37] Nordic Semiconductors, "$\lambda/4$ printed monopole antenna for 2.45 GHz," *January*, 2005.

[38] Coilcraft Inc., "Measuring Self-Resonant Frequency," *Document 363-1*, vol. 5, no. 4, pp. 1–3, 2004.